



Characterisation of *Plin4* null mice

Absence of *Plin4* results in
lower hepatic expression of
genes involved in
lipogenesis

Master Thesis by
Ingvild Solberg Kvam

Department of Nutrition
Faculty of Medicine
University of Oslo
May 2019

Characterisation of *Plin4* null mice

Absence of Plin4 results in lower hepatic expression of genes involved in lipogenesis

Ingvild Solberg Kvam



Master Thesis
Department of Nutrition
Faculty of Medicine

UNIVERSITY OF OSLO

May 2019

© Ingvild Solberg Kvam

2019

Characterisation of *Plin4* null mice – Absence of *Plin4* results in lower hepatic expression of genes involved in lipogenesis

Ingvild Solberg Kvam

<http://www.duo.uio.no/>

Print: Reprosentralen, Universitetet i Oslo

II

Abstract

Introduction: Lipid droplets (LDs) are highly dynamic cellular organelles with a core of neutral lipids, surrounded by phospholipids and proteins. The perilipin proteins (Plins) serve as key components in the LD surface and are important for stabilisation of the neutral LD core. Five Plins are identified to be associated to the LD surface. The function of Plin4 is poorly understood and have been investigated in this master thesis.

Materials and methods: The role of *Plin4* was investigated in adipose tissue and liver under fed and fasted conditions by comparing *Plin4*^{+/+} and *Plin4*^{-/-} mice. Mice have been exposed to two separate diet interventions, high-fat diet and Western diet, along with corresponding control diets. The diet interventions lasted for ~10 weeks, from the mice were 8 weeks of age until 18 weeks of age. In a third intervention, mice were exposed to food deprivation for 24 hours and compared to a fed state. At the end of all interventions, dissected tissues were collected for further analyses. Molecular analyses performed in this thesis has focused on gene expression analysis, LD visualisation, and measurement of the content of triacylglycerol (TAG) and total cholesterol in liver and adipose tissue. Quantitative reverse transcription polymerase chain reaction (RT-qPCR) was used for gene expression analyses on total ribonucleic acid (RNA) samples. Colorimetric kits were used to measure content of TAG and total cholesterol in homogenate of liver tissue. Liver tissue embedded in Optimal Cutting Temperature (OCT) medium was used to generate cryosections for histological examination.

Results: The main finding presented in this master thesis was lower expression of genes involved in hepatic lipogenesis in mice lacking functional *Plin4*. This reduction was seen in *Plin4*^{-/-} female mice receiving Western control diet and *Plin4*^{-/-} male mice receiving chow diet. Secondly, significantly lower expression of *Plin5* in liver were seen in *Plin4*^{-/-} male mice receiving high-fat diet, *Plin4*^{-/-} female mice receiving Western control diet and fasted *Plin4*^{-/-} male mice. Lastly, mice lacking *Plin4* show altered hepatic response to fasting. Fasted *Plin4*^{-/-} mice have significantly lower expression of *Ppara* and reduced accumulation of TAG in liver, compared to fasted *Plin4*^{+/+} mice.

Conclusion: Expression of genes involved in hepatic lipogenesis were lower when *Plin4* was absent. Expression of *Plin5* in liver was reduced in *Plin4*^{-/-} mice compared to *Plin4*^{+/+} mice. Mice lacking *Plin4* have altered response to fasting.

Acknowledgements

This master thesis has been conducted at the Department of Nutrition, Faculty of Medicine at the University of Oslo, from August 2018 to May 2019. The work has been carried out in the Norwegian Transgenic Centre (NTS). Several individuals have contributed to make this year very special to me and guided me through every step of the way.

First, I would like to thank the Lipid droplet research group for the warm welcome to the group and for including me in all your research discussions. I have learned so much of you all and have been able to evolve in scientific thinking, which has been really valuable to me.

I would like to give a special thanks to my supervisors, Knut Tomas Dalen and Frode Norheim, for your wise guidance, your patience and instructive feedback through the whole process. I have always felt welcome in your offices and you've both given priority to discuss and guide me. I am forever grateful for that. I would also like to thank Ingunn Jermstad and Shaista Khan, for all your support and nice talks, and PhD Yuchuan Li, for your laboratory guidance throughout the project, and especially with all your help in histology work.

I would also like to thank my dearest friend, Maria Fossli. Words cannot describe how much you mean to me. You've been my rock throughout this whole year and without you by my side – for limitless support and the best lunch breaks, this year wouldn't have been the same.

Most of all, I would like to thank my mum and dad, for helping out with the kids through the final of this master thesis and for always giving me tons of support. And Eleah and Liam, for giving me the best hugs and kisses, and for coping with your stressed mum the last weeks until delivery. You both have been the greatest motivation to me and I cannot wait to finally be able to keep my shoulders down and be the best mum I can possibly be to you both.

The most special thank you goes to Peter, my loving husband, for all your patience, guidance and support, even though cancer treatment has been keeping you down for the last couple of months. Your support means the world to me and I could not have finished this without you by my side.

List of abbreviations

ABCA/G / <i>Abca/g</i>	ATP-binding cassette subfamily A and G / <i>gene</i>
ANOVA	Analysis of variance
ApoE / <i>ApoE</i>	Apolipoprotein E / <i>gene</i>
ATGL	Adipose triglyceride lipase
ATP	Adenosine triphosphate
BAT	Brown adipose tissue
BMI	Body mass index
cAMP	Cyclic adenosine monophosphate
cDNA	Complementary DNA
CE	Cholesteryl ester
ChREBP / <i>ChREBP</i>	Carbohydrate response element binding protein / <i>gene</i>
CO₂	Carbon dioxide
DNL	<i>De novo</i> lipogenesis
DAG	Diacylglycerol
DGAT / <i>Dgat</i>	Diacylglycerol acyltransferase / <i>gene</i>
DNA	Deoxyribonucleic acid
dNTP	Deoxynucleoside triphosphate
EtOH	Ethanol
FASN / <i>Fasn</i>	Fatty acid synthase / <i>gene</i>
HMG-CoA	3-hydroxy-3-methylglutaryl coenzyme A
HSL	Hormone sensitive lipase
LD	Lipid droplet
LDL-R / <i>Ldlr</i>	Low-Density lipoprotein receptor / <i>gene</i>
LPL / <i>Lpl</i>	Lipoprotein lipase / <i>gene</i>
LXR / <i>Lxr</i>	Liver X receptor / <i>gene</i>
MAG	Monoacylglycerol
MGL	Monoacylglycerol lipase
mRNA	Messenger ribonucleic acid
NAFLD	Non-alcoholic fatty liver disease
NaN₃	Sodium azide

NaPi	Sodium Phosphate buffer
NASH	Non-alcoholic steatohepatitis
NEFA	Non-esterified fatty acid
OCT	Optimal cutting temperature
PBS	Phosphate-buffered Saline
PFA	Paraformaldehyd
PKA	Protein kinase A
<i>Plin1 / Plin1</i>	Perilipin 1 protein / <i>gene</i>
<i>Plin2 / Plin2</i>	Perilipin 2 protein / <i>gene</i>
<i>Plin3 / Plin3</i>	Perilipin 3 protein / <i>gene</i>
<i>Plin4 / Plin4</i>	Perilipin 4 protein / <i>gene</i>
<i>Plin5 / Plin5</i>	Perilipin 5 protein / <i>gene</i>
PPAR / <i>Ppar</i>	Peroxisome proliferator-activated receptor / <i>gene</i>
PPRE	PPAR response element
RNA	Ribonucleic acid
RPM	Revolutions per minute
RT	Reverse transcriptase
RT-qPCR	Quantitative reverse transcription polymerase chain reaction
RXR	Retinoid X receptor
SEM	Standard error of the mean
SREBP / <i>Srebp</i>	Sterol regulatory element binding protein / <i>gene</i>
TAG	Triacylglycerol
TBP	TATA binding protein
UCP1	Uncoupling protein 1
VLDL	Very-low-density lipoprotein
WAT	White adipose tissue
WHO	World Health Organization

List of tables

Table 1.	Kits
Table 2.	Equipment
Table 3.	Chemicals and reagents
Table 4.	Software's and internet resources
Table 5.	Diet compositions and mice included in this study
Table 6.	Tissue homogenization for RNA isolation
Table 7.	Recipe, high salt buffer
Table 8.	Recipe, reverse transcriptase master-mix
Table 9.	Recipe, master-mix for RT-qPCR
Table 10.	Recipe, cryoprotection solution
Table 11.	Staining solution
Table 12.	Mice characteristics after ~10 weeks of a high-fat diet intervention
Table 13.	Mice characteristics after ~10 weeks of a western diet intervention
Table 14.	Mice characteristics in mice receiving chow diet and fasted for 24 hours

List of figures

- Figure 1.** Gene expression of Plin family members, epididymal fat, high-fat diet intervention
- Figure 2.** Hepatic gene expression of Plin family members, high-fat diet intervention
- Figure 3.** Hepatic gene expression of Plin family members, western diet intervention
- Figure 4.** Hepatic expression of genes involved in lipid metabolism, western diet intervention
- Figure 5.** Hepatic content of triacylglycerol and total cholesterol, western diet intervention
- Figure 6.** Histological appearance of hepatic lipid content, western diet intervention
- Figure 7.** Amount of epididymal fat and weight loss, fasting intervention.
- Figure 8.** Hepatic gene expression of Plin family members, fasting intervention
- Figure 9.** Hepatic expression of genes involved in lipid metabolism, fasting intervention
- Figure 10.** Hepatic content of triacylglycerol and total cholesterol, fasting intervention

List of appendices

Appendix 1. Specific primer-pairs used for RT-qPCR

Table of content

List of abbreviations.....	V
List of tables.....	VII
List of figures	VIII
List of appendices.....	IX
1 Introduction	1
1.1 Adipose tissue.....	1
1.1.1 Obesity	2
1.2 Liver.....	3
1.2.1 Non-alcoholic fatty liver disease.....	4
1.3 Lipid metabolism.....	4
1.3.1 Lipogenesis.....	4
1.3.2 Lipolysis	5
1.3.3 Transcription factors regulating lipid metabolism	6
1.4 Lipid droplets.....	7
1.5 Perilipin proteins.....	8
1.5.1 Plin1	8
1.5.2 Plin2	9
1.5.3 Plin3	9
1.5.4 Plin4	9
1.5.5 Plin5	10
1.6 Aims.....	11
2 Material and Methods.....	12
2.1 Material.....	12
2.1.1 Material used for data collection and molecular analyses.....	12
2.1.2 Animal models and diet interventions.....	14
2.2 Methods	15
2.2.1 Animal experiments	15
2.2.2 Quantitative reverse transcription polymerase chain reaction	16
2.2.3 Measuring hepatic content of triacylglycerol and total cholesterol	19
2.2.4 Histological examination.....	20
2.2.5 Statistical methods.....	22

3	Results	23
3.1	High-fat diet intervention	23
3.1.1	Mice characteristics	23
3.1.2	Gene expression analysis	24
3.2	Western diet intervention.....	27
3.2.1	Mice characteristics	27
3.2.2	Gene expression analysis	28
3.2.1	Content of triacylglycerol and total cholesterol	32
3.2.2	Histology	33
3.3	Fasting	34
3.3.1	Mice characteristics	34
3.3.2	Gene expression	36
3.3.3	Content of triacylglycerol and total cholesterol	39
4	Discussion	40
4.1	Discussion of the methodology	40
4.1.1	Animal knock-out models	40
4.1.2	Quantitative reverse transcription polymerase chain reaction	41
4.1.1	Measuring hepatic content of triacylglycerol and total cholesterol	42
4.1.2	Histology	43
4.1.3	Statistical methods and sample size	44
4.2	Discussion of the results	45
4.2.1	Main results	45
4.2.2	Clinical relevance	47
5	Conclusion.....	49
	References	51
	Appendix	57

1 Introduction

1.1 Adipose tissue

Metabolic health is dependent on the body's ability to balance fluctuations in availability and requirement of energy. Because of its high content of energy, triacylglycerol (TAG) serves as the major energy source in most organisms (1). Adipose tissue serves as the major reservoir of energy in the form of TAG for the human body (2). Energy is mobilised from adipose tissue and secreted as non-esterified fatty acids (NEFAs) and glycerol when the requirement of energy accrues.

In mammals there are two types of adipose tissue with adipocytes that differ in morphology and function. Brown adipose tissue (BAT) is a highly oxidative tissue (2, 3) specialised in thermogenesis and contains abundant amounts of mitochondria that generate heat by oxidising fatty acids combined with uncoupling of the electron transport chain via uncoupling protein 1 (UCP1) (2-5). BAT store energy in the form of neutral lipids, mainly TAG, but in lesser amount compared to white adipose tissue (WAT).

WAT is widely distributed in the whole body, mostly consisting of adipocytes (6). The main purpose of WAT is to store energy, and the adipocytes have a unique capability to store large amounts of energy as neutral lipids (7, 8). These neutral lipids serve as the buffering system for lipid energy balance by being taken up and released dependent on the organisms energy demand (2, 9). The NEFAs are primarily released from adipose tissue when the body's need for energy is high and the level of insulin is low, like during fasting (5, 10).

WAT is not a uniform tissue but is divided into fat depots that differ in anatomical location, structural organisation, size of the adipocytes and biological function (11). The largest fat depots are found subcutaneously and round viscera (6). The subcutaneous fat depots have the greatest storing capacity and provide an important buffering function for storage of energy (11). The visceral fat depots are found deeper in the body and surround internal organs (6). Visceral fat are more metabolically active than the subcutaneous fat (11), and takes up released NEFAs to buffer nutrient supply during and after a meal.

Although adipocytes are specialized for storing lipids (1), chronic overfeeding may overload this storing capacity and the pool of NEFAs inside cells and in the circulation will increase

(11). Excess lipids will then be stored in visceral fat depots (11) and in non-adipose tissue such as liver and muscle (1). Increasing visceral fat mass are strongly associated with increased risk of type 2 diabetes and cardiovascular disease (5, 11). The non-adipose storage is often referred to as ectopic fat (12) and is associated with co-morbidities associated with obesity (5) in the same manner as visceral fat depots (11, 13). The distribution of fat between subcutaneous and visceral fat depots differ between gender, age and genetic components, and this distribution seems to be the most decisive risk factor for the development of obesity-related diseases (11). Understanding the regulation of lipid metabolism and the accumulation of lipids in non-adipose tissues will help us understand the mechanisms behind the onset of metabolic diseases.

1.1.1 Obesity

According to the World Health Organization (WHO), obesity has nearly tripled the last four decades and is often referred to as the “global obesity epidemic” (14). This dramatic increase is seen in both developed and developing countries (15), and globally there are now more people that are overweight or obese, than normal weight or underweight (14, 15). The fundamental cause of overweight and obesity is an imbalance between energy consumption and energy expenditure (13) which results in expanding adipose tissue depots and potentially deposition of lipids in non-adipose tissues (13). The obesity epidemic is caused by changes in lifestyle and dietary habits, consisting of a sedentary lifestyle and dietary excess of energy-dense food (1, 15).

Adverse alterations of the adipose tissue are observed in relation to obesity. In obese individuals, the adipocyte storing capacity can be exceeded, and the adipose tissue take up less NEFAs than usual, and also leak NEFAs to the circulation (15). Inflammation is also associated with obesity. Increased inflammatory activity results in tissue infiltration of macrophages, which secrete inflammatory cytokines that are found to interfere with different metabolic pathways (16). Inflammation is the major contribution to co-morbidities related to obesity, such as cardiovascular disease, hypertension, dyslipidaemia, hepatic steatosis, insulin resistance, hyperglycaemia and type 2 diabetes (17). These are all non-communicable diseases characterised by high accumulation of TAG in non-adipose tissues (1).

1.2 Liver

The liver is the largest abdominal organ and weighs approximately 1500 grams in a human adult (18). The organ is located in the upper right part of the abdominal cavity, below the diaphragm (19), where it takes up most of the space under the ribs. Underneath the right side of the liver, the gall bladder, parts of the pancreas and the intestines are connected to the liver surface (19). The liver carries out a variety of important metabolic functions in tight collaboration with the gall bladder, pancreas and the intestines.

From a histological view, the liver tissue is divided into hexagonal lobules with parts of the portal vein, the hepatic artery and biliary ducts in each corner of each lobule (18). These three structures are referred to as the portal triad. The central veins are found in the centre of each lobule. The liver receives blood from the hepatic artery derived from the aorta, and from the portal vein, which collects blood drained from the digestive tract (19).

The liver is central in the carbohydrate and lipid metabolism. Under fed conditions, where the body is in energy surplus and insulin levels are high, the liver receives nutrients from the food we ingest (20). The portal vein provides the liver with a different range of nutrients including carbohydrates and short chain fatty acids, while long-chain fatty acids are delivered to the periphery before some of it eventually reach the liver as chylomicron remnants (19).

Nutritional overload with carbohydrates and subsequently high levels of insulin promote glycogen synthesis and *de novo* lipogenesis, resulting in an incorporation of glucose into glycogen and fatty acids into TAG (20). Most of the energy needed for the body to drive different metabolic processes under fed conditions, is received through active glycolysis in liver (21).

Under fasted conditions, where the body is in energetic need, the liver receives NEFAs secreted from adipose tissue due to active lipolysis in adipocytes (22). In response to lack of insulin and simultaneously high levels of stored glycogen, the liver downregulates glycolysis, activates gluconeogenesis, and switch to generate its own energy from oxidation of the NEFAs received from the circulation. The flux of NEFAs through the β -oxidation is high, and the produced acetyl-CoA (oxidation product) are fully oxidised to carbon dioxide (CO₂) in the Krebs cycle (21). This generates abundant amounts of adenosine triphosphate (ATP), which promotes the conversion of pyruvate, glycerol or three-carbon molecules into glucose via gluconeogenesis (21). If the oxidative capacity of the Krebs cycle is exceeded, excess acetyl-

CoA is converted into ketone bodies that are secreted from the liver to provide energy in other tissues (21).

1.2.1 Non-alcoholic fatty liver disease

Non-alcoholic fatty liver disease (NAFLD) refers to a group of conditions where excess fat is accumulating in the liver. It is the most common liver disorder worldwide and the leading cause of chronic liver disease in the western part of the world (10, 23, 24). NAFLD is more common among individuals with body mass index (BMI) above 30 kg/m² (11) and the incidence and prevalence are rising with increasing rates of obesity (24).

In NAFLD, the hepatic uptake of fatty acids and the *de novo* lipogenesis (DNL) are increased beyond normal physiology, and oxidation of fatty acids are insufficient to maintain balanced hepatic lipid levels (25). As a result, hepatic lipids accumulate in unhealthy proportions (25). This abnormal hepatic lipid metabolism is found to be closely related to many non-communicable diseases (25), insulin resistance (11), and development of fibroses in the liver (10), which might result in non-alcoholic steatohepatitis (NASH) and cirrhosis.

1.3 Lipid metabolism

Lipid metabolism is a dynamic process that involves the constant flow of lipids derived from the diet, delivered to the liver and peripheral tissues, and the flow from the periphery and back to the liver. The lipid metabolism involves many different enzymes for degradation and synthesis of lipids, and a range of proteins to transport the hydrophobic lipid molecules in the circulation and through lipid membranes. The molecular pathways in lipid metabolism involves the synthesis of fatty acids and neutral lipids such as TAG (lipogenesis) (26), degradation of neutral lipids (lipolysis) (27) and oxidation of fatty acids (β -oxidation) (28). Some of these pathways, relevant for this master thesis, will be described below.

1.3.1 Lipogenesis

Lipogenesis involves synthesis of fatty acids and subsequent synthesis of TAG. Lipogenesis is initiated in liver and adipose tissue when surplus energy is available (26). Fatty acids may be derived from dietary intake of fat or by the *de novo* synthesis of fatty acids from excess of carbohydrates. A diet rich in fat decreases expression of genes involved in hepatic lipogenesis

and lowers the lipogenesis in liver (26), while it promote fatty acid uptake, lipogenesis and lipid storage in adipose tissue. A diet rich in carbohydrates has the opposite effect in liver, initiating the *de novo* synthesis of fatty acids from excess carbohydrates (10), whereas it stimulates lipogenesis in both liver and adipose tissue (26). Fatty acids may undergo desaturation, elongation or esterification before being used in synthesis of TAG for hepatic storage or transportation in very-low-density lipoprotein (VLDL) particles to the periphery (25).

During fasting, the lipogenesis in adipose tissue is reduced and lipolysis is activated to release stored TAG as NEFAs and glycerol (22). NEFAs are released from adipose tissue and taken up by hepatocytes to provide energy, and being substrates for hepatic synthesis of TAG for storage and release to the periphery (26). The diacylglycerol acyltransferase (DGAT) enzymes, DGAT1 and DGAT2, are involved in the synthesis of TAG by catalysing the adding of a fatty acid to diacylglycerol (DAG) (29). The produced TAG is stored in hepatocytes or released from the liver incorporated into VLDL particles (10).

1.3.2 Lipolysis

Lipolysis is defined as the sequential hydrolysis of TAG into glycerol and three NEFAs, providing fatty acids as a major fuel source for mitochondrial β -oxidation in times of energetic need (27, 28). Lipolysis occurs in the gastrointestinal lumen, in the blood vessels and intracellularly in nearly all cells (27). Intracellular lipolysis in hepatocytes and adipocytes will be further described.

The hydrolytic process of lipolysis is mediated by three different enzymes: the adipose triglyceride lipase (ATGL), the hormone sensitive lipase (HSL) and the monoacylglycerol lipase (MGL). These enzymes catalyse the hydrolysis of TAG in response to fasting and/or lack of nutrients (27, 30). In the first step of lipolysis, TAG is hydrolysed to DAG and one free fatty acid. This reaction is mainly catalysed by ATGL (31). By the action of HSL, DAG is converted to monoacylglycerol (MAG) and a free fatty acid. Finally, MAG is converted to glycerol and a third free fatty acid. This last step is catalysed by MGL (9). These enzymes work independently and lipolysis may be incomplete and terminated at the described intermediates. Nevertheless, the first step catalysed by ATGL is the rate-limiting step. ATGL requires a co-activator protein to obtain fully hydrolytic activity (31). The association of this co-activator protein, termed Abhd5/CGI-58, enhances the hydrolysis of TAG by 20-fold

compared to the action of ATGL alone (31), and thereby promotes lipolysis and lowers lipid storage.

In basal conditions (fed state) when the availability for energy is high and the need for energy is covered by external sources, the rate of lipolysis in adipocytes is low and lipid storage dominates. Insulin levels are elevated in a fed state, resulting in repression of the lipolysis in the adipocytes (32). In basal conditions, CGI-58 is associated with protein and ATGL remains inactive (33, 34). HSL is found in the cytosol in an un-phosphorylated, inactive state (35, 36).

In stimulated conditions (fasted state), the need for energy is high and the cell is stimulated by catecholamine hormones, leading to a series of intracellular reactions that ends with the activation of the cyclic adenosine monophosphate (cAMP) dependent protein kinase A (PKA) (35, 36). PKA promotes the phosphorylation of CGI-58 (37), HSL (36) and associated proteins (38). This phosphorylation is decisive for the translocation of HSL from the cytosol to the LD surface to participate in the lipolysis (12, 39), and for the release of CGI-58 (40). When released, CGI-58 binds to and co-activates ATGL (35, 41). When associated with CGI-58, ATGL initiates the lipolysis by the hydrolysis TAG to DAG. HSL continues the breakdown of TAG before MGL completes the lipolysis.

The NEFAs derived from the lipolysis have different routes for usage. They are either released to the bloodstream bound to albumin and transferred to the liver for distribution in VLDL particles to different tissues, or kept inside the cell to act as signal molecules or gene transcription regulators (27). Intracellular NEFAs may also be re-esterified to TAG (27, 28).

1.3.3 Transcription factors regulating lipid metabolism

Expression of enzymes catalysing lipogenesis and oxidation of fatty acids are regulated by several transcription factors, including peroxisome proliferator-activated receptors (PPARs), liver X receptors (LXRs), carbohydrate response element binding protein (ChREBP) and sterol regulatory element-binding proteins (SREBPs). PPARs are a nuclear receptor family consisting of the isotypes PPAR α , PPAR β/δ and PPAR γ with specific tissue distribution, regulating genes involved in the metabolism of lipids and carbohydrates (11, 42). The PPARs are ligand-activated by fatty acids or metabolic derivatives of fatty acids (11). When bound and activated by ligand, the PPAR heterodimers with retinoid X receptor (RXR) and binds to the PPAR response element (PPRE) in the gene regulating regions of target genes and increase

the expression of these target genes (42). PPAR α is mainly involved in the regulation of genes related to beta-oxidation (43), PPAR γ is involved in adipogenesis and lipid metabolism (44), while the function of PPAR β/δ is less understood.

LXRs are nuclear receptors consisting of LXR α and LXR β , which are involved in cholesterol, carbohydrate and lipid metabolism (45, 46). These nuclear receptors are sterol dependent and activated by oxysterols (46). LXR target genes include *ATP-binding cassette subfamily A and G (Abca and Abcg)*, *Srebp1c*, *Fatty acid synthase (Fasn)*, *Lipoprotein lipase (Lpl)* and *Apolipoprotein E (ApoE)* (46, 47).

ChREBP is a helix-loop-helix leucine zipper transcription factor that regulates expression of genes involved in hepatic lipogenesis (48). The function of ChREBP is glucose-dependent. Target genes for ChREBP include *Pyruvate kinase* and *Fasn*, and the main role of ChREBP is the conversion of excess glucose into fatty acids for storage as TAG (48).

SREBPs are a transcription factor family consisting of three isoforms that regulates the expression of genes involved in the synthesis of cholesterol, fatty acids, TAG and phospholipids (49, 50). Srebp1a is found to be involved in the regulation of genes involved in the synthesis of both cholesterol and fatty acids, for example *3-hydroxy-3-methylglutaryl-coenzyme A (HMG-CoA) synthase* and *Fasn*. Srebp1c is found to selectively induce the expression of lipogenic genes, while *Srebp2* regulates genes involved in the cholesterol synthesis (49).

1.4 Lipid droplets

All eukaryotic cells have the ability to store lipids in cytosolic lipid droplets (LDs) (51), but their capacity to synthesise LDs varies (52). The LDs differ in size, number, interaction with other organelles, and localisation in the cell (52, 53). Mammalian LDs have the ability to store fatty acids and sterols as TAG and cholesteryl esters (CE), respectively (54), and to rapidly mobilise these stored lipids when needed.

The compartmentalisation of neutral lipids into LDs for storage protect peripheral tissues from overload of free lipids in the cytosol (54). An imbalance in this lipid storage is associated with a number of human metabolic diseases (9, 52). Increased understanding of the biology of LDs is therefore of great importance.

LDs are highly dynamic cellular compartments (54). They contain a core of neutral lipids surrounded by a monolayer of phospholipids and cholesterol, and structural and regulatory proteins (12, 55, 56). The first mammalian protein identified to be associated to the LD surface was perilipin (Plin) (57). Further research revealed four additional proteins with sequence similarity within the N-terminal region of the first discovered Plin (54). Due to the names of the three initial proteins discovered (**P**erilipin, **A**DRP and **T**ip47), these proteins were originally referred to as the PAT-domain proteins (58-60). With the discovery of the two latest members, a uniform nomenclature was proposed where the Plin family members were numbered according to the order they were discovered: Plin1 (peri or perilipin) (57), Plin2 (ADRP, ADFP or adipophilin) (61), Plin3 (pp17 or Tip47) (62), Plin4 (S3-12) (63) and Plin5 (Lsd5, Mldp or oxPAT) (64), respectively.

1.5 Perilipin proteins

The Plins serve as key components of the LD surface (54, 55, 65) where they are believed to stabilise the surface and protect neutral lipids in the core from lipolytic degradation (1, 58). The Plins differ in tissue expression and binding-affinity to LDs (54) which suggests differences in function. Some Plins are expressed ubiquitously, while others are expressed in specific cell types (8, 52, 55, 65). Certain Plins show specific preferences for separate pools of LDs, depending on the lipid composition of neutral lipids accumulated in the LD core (66).

1.5.1 Plin1

Plin1 is the most studied Plin protein and is exclusively associated with LDs (67). The Plin1 gene (*Plin1*) gives rise to four different protein isoforms (Plin1a-d) with different preference for LDs with TAG or CE in the core (66). It is highly expressed in adipose tissue and in lower levels in steroidogenic cells (38, 59). Plin1 serves as a key regulator of lipolysis in adipocytes and the absence of *Plin1* results in increased basal lipolysis (67, 68), which confirms its protective role in repressing the hydrolysis of stored lipids. Mice with absence of *Plin1* are resistant to diet-induced obesity due to increased metabolic rate (69). The Plin1 is targeted for PKA-mediated phosphorylation (70) and its phosphorylated state is important for its protective role in repressing the lipolysis (69).

1.5.2 Plin2

Plin2 is expressed in most cell types and is exclusively associated with LDs in the same way as Plin1 (55, 61). Plin2 show no specific preference for LDs with either TAG or CEs in the core, and therefore binds different LDs with similar affinity (66). Plin2 is involved in the formation of LDs and in hepatic lipid storage. Absence of *Plin2* reduces accumulation of TAG in liver by increasing secretion of VLDL particles (71, 72). Studies suggest that the absence of *Plin2* protects against diet-induced fatty liver disease (72). Plin2 is not target for PKA-mediated phosphorylation under stimulated lipolysis (70) and the role in regulating the lipolysis is unclear.

1.5.3 Plin3

Plin3 is ubiquitously expressed and is found stable both as a soluble protein in the cytoplasm and associated to the LD surface (55, 62, 73). Plin3 show no specific preference for LDs with either TAG or CEs in the core (66), and no clear regulation mechanism is found for *Plin3*. The function of Plin3 is poorly understood and its involvement in the regulation of lipolysis is unclear. Absence of *Plin3* is found to change LD morphology (74) and mice lacking *Plin3* is more cold tolerant than mice with functional *Plin3*. The mechanism is although unclear.

1.5.4 Plin4

Plin4 is highly expressed in adipose tissue (75), and to some degree in oxidative tissues such as skeletal muscle (75) and in the heart (63, 76). Plin4 is found stable both associated to the LD surface and in the cytoplasm (55). Plin4 shows a specific preference for LDs rich in CEs (66). While the four other Plin family members show sequence similarity in the amino terminus, Plin4 has divergent amino acid sequence and share only sequence similarity in intermediary 11-mer repeat region (55). Plin4 show no involvement in the regulation of lipolysis in adipocytes and is not required for optimal function of Plin1 (76). Absence of *Plin4* have shown to reduce cardiac accumulation of TAG (76), but the physiological role of *Plin4* is still poorly understood. There is previously shown that lack of *Plin4* in mice reduces the expression of *Plin5* in heart and liver (76). Further investigation is needed to identify the specific function of Plin4, which is the main purpose of this master thesis.

1.5.5 Plin5

Plin5 is mainly expressed in tissues with high levels of fatty acid oxidation, such as heart, skeletal muscle and fasting liver (64). The protein is found stable bound to the LD surface as well as soluble in the cytoplasm (55, 77). Plin5 shows a specific preference for LDs rich in TAG (66). Plin5 is target for PKA-mediated phosphorylation (55) and represses lipolysis in the heart by interacting with CGI-58 and limiting its association with ATGL (78, 79). The absence of *Plin5* reduce the lipid content in the heart and reduce the size and number of LDs (78, 80, 81), indicating an increased turnover of lipids in the absence of *Plin5*, particularly in the heart.

1.6 Aims

This master thesis is part of a larger project studying the roles of Plins. The Lipid droplet research group has previously characterised transcriptional regulation of *Plin4*. The primary objective of this master thesis was to investigate the role of *Plin4* in lipid metabolism by studying biological material collected from *Plin4*^{+/+} and *Plin4*^{-/-} mice.

The specific aims of this master thesis are as follows:

1. Compare expression of genes involved in lipid metabolism in *Plin4*^{+/+} and *Plin4*^{-/-} mice receiving various diets
2. Compare expression of other Plin family members in *Plin4*^{+/+} and *Plin4*^{-/-} mice receiving various diets
3. Investigate the response to fasting in *Plin4*^{+/+} and *Plin4*^{-/-} mice by comparing gene expression and hepatic lipid content
4. Compare mice characteristics such as body weight, organ weight and lipid composition in *Plin4*^{+/+} and *Plin4*^{-/-} mice receiving various diets or food withdraw (fasting)

2 Material and Methods

2.1 Material

2.1.1 Material used for data collection and molecular analyses

Kit	Producer
Cholesterol 1600, ERBA Diagnostics	MaxMat SA (Montpellier, France)
High-Capacity cDNA Reverse Transcription kit	Applied Biosystems (Warrington, UK)
NucleoSpin RNA kit	Macherey-Nagel (Düren, Germany)
Trigalycérides Enzymatique PAP 150 (TG PAP 150)	Biomérieux (Rue Censier, France)

Table 1. Kits. This table presents all kits (with producer) used for data collection and molecular analyses performed in this master thesis.

Equipment	Producer
ABI Prism 96-Well Optical Reaction Plate	Applied Biosystems (Foster City, US)
ABI Prism Optical Adhesive sealing	Applied Biosystems (Foster City, US)
BioTek SYNERGY H1 microplate reader	TermoFisher Scientific (Waltham, MA, USA)
Centrifuge, Biofuge fresco	Kendro Laboratory (Tyskland)
Centrifuge, Mini Spi, Eppendorf	Eppendorf AG (Hamburg, Tyskland)
Centrifuge, Mini Spi, PCR strips	TermoFisher Scientific (Waltham, MA, USA)
CFX96 Real-Time System Thermal Cycler	Bio-Rad Laboratories (Hercules, CA, US)
Cryostat CM3050S	Leica Biosystems (Newcastle, UK)
Embedding molds	Sigma (St. Louis, MO, US)
Eppendorf tubes	Sarstedt (Germany)
Falcon tubes	Falcon, Corning Incroporation (Durham, US)
Filter paper	Bio-Rad Laboratories (Hercules, CA, US)
Glass beads (1 mm)	Glass beads, Assistent, (Tyskland)
Gloves	Kimtech, Kimberly-Clark Professional
Mastercycler Ep Gradient S	Eppendorf AG (Hamburg, Tyskland)
Microseal, B' Adhesive Seals For PCR Plates	Bio-Rad Laboratories (Hercules, CA, US)
Micro tubes	Sarstedt (Germany)
Multi-channel pipette	Eppendorf research (Germany)
NanoDrop-1000 Spectrophotometer	TermoFisher Scientific (Waltham, MA, USA)
PCR strips with attached caps	TermoFisher Scientific (Waltham, MA, USA)
Pipette tips, Biosphere (5 ml, 10 ml, 25 ml)	Falcon, Corning Incroporation (Durham, US)
Pipetboy acu 2	Integra Bioscience (Hudson, US)
PreLys24 Homogenizer	Bertin Instruments (France)
SuperFrost® Plus Microscope Slides	TermoFisher Scientific (Waltham, MA, USA)
Well plate (12 wells)	Sigma (St. Louis, MO, US)

Table 2. Equipment. This table consists of all equipment (with producer) used for data collection and molecular analyses performed in this master thesis.

Chemicals and reagents	Producer
Beta-mercaptoethanol	Sigma (St. Louis, MO, US)
Bodipy (493/503) 1 mM	Invitrogen (Life technologies, Paisley, UK)
Chow diet	Research Diets INC (US)
Dry ice	Praxair (Guildford, UK)
Ethanol (EtOH) 96 %	Sigma (St. Louis, MO, US)
Ethylene glycol	Sigma (St. Louis, MO, US)
High fat diet	Research Diets INC (US)
High-fat control diet (low-fat diet)	Research Diets INC (US)
Hoechst 20 mM	Sigma (St. Louis, MO, US)
Liquid nitrogen	Praxair (Guildford, UK)
Optimal Cutting Temperature (OCT) media	Cell Path (Newtown Powys, Mid Wales, UK)
Paraformaldehyde (PFA) 0.4 %	Sigma (St. Louis, MO, US)
Phalloidon CF568-conjugate 200 U/mL	Invitrogen (Life technologies, Paisley, UK)
Phenol:Chloroform:Isoamylalcohol (24:24:1)	Invitrogen (Life technologies, Paisley, UK)
Phosphate-buffered saline (PBS)	Sigma (St. Louis, MO, US)
Polyvinyl-pyrrolidone (PVP-40)	Sigma (St. Louis, MO, US)
Primers (<i>see appendix 1</i>)	Sigma (St. Louis, MO, US)
ProLong™ Diamond Antifade Mountant	TermoFisher Scientific (Waltham, USA)
Sodium acetate (CH ₃ COONa)	Sigma (St. Louis, MO, US)
Sodium Azide (NaN ₃)	Sigma (St. Louis, MO, US)
Sodium chloride (NaCl)	Sigma (St. Louis, MO, US)
Sodium Phosphate buffer (NaPi) 0,1M	Sigma (St. Louis, MO, US)
SsoAdvanced Universal SYBR Green Supermix	Bio-Rad Laboratories (Hercules, CA, US)
Sucrose 10, 20 and 30 %	Sigma (St. Louis, MO, US)
Western diet	Research Diets INC (US)
Western control diet	Research Diets INC (US)

Table 3. Chemicals and reagents. This table consists of all chemicals and reagents (with producer) used in the data collection and molecular analyses performed in this master thesis.

Program	Producer
Adobe Illustrator CS6	Adobe (San Jose, CA, US)
Confocal Software: ZEN 2.3 (blue edition)	Carl-Zeiss Microscopy GmbH (Jena, Germany)
EndNote X9	Thomson Reuters
Gen5 2.06	BioTek Instruments, Inc
GraphPad Software	GraphPad Software Inc. (San Diego, CA, USA)
Microsoft Office 2010	Microsoft®
ND-1000 Software	Saveen & Werner AB, Sweden
7900 SDS v2.3	TermoFisher Scientific (Waltham, MA, USA)

Table 4. Software's and internet resources. This table consists of software's and internet resources (with producer) used for data collection and processing in this master thesis.

2.1.2 Animal models and diet interventions

The Lipid droplet research group is currently characterising mice lacking a functional *Plin4* gene (*Plin4*^{-/-} mice), and this master thesis has been a part of this larger project. *Plin4*^{-/-} mice were generated using the standard gene disrupting method in embryonic stem cells and the obtained *Plin4*^{-/-} mouse has later been backcrossed to a congenic strain (the C57BL/6N strain) for at least ten generations. *Plin4*^{+/+} and *Plin4*^{-/-} mice from the same breeding colony have been used in this study. All procedures were performed in accordance to the guidelines for care and use of experimental animals in Directive 2010/63/EU of the European Parliament, on the protection of animals used for scientific purposes. The mice were housed in cages of 3-4 animals, in a temperature controlled facility at 22°C with a strict 12 hours light/dark cycle.

Plin4^{+/+} and *Plin4*^{-/-} mice were included in a high-fat diet intervention, a Western diet intervention, and a fasting intervention. The mice were given free access to chow food (consisting of 58 E% carbohydrates, 18 E% fat and 24 E% protein) until initiation of diet interventions (diets from Research Diets, Inc, USA). All mice had free access to water prior to and during diet interventions, except for the fasting period in the fasting intervention. At the end of all three interventions, mice were euthanized by cervical dislocation. Bodyweight was measured before and after 24 hours of fasting for the mice in the fasting intervention, and for all mice right after euthanasia. Tissues were dissected, and organ weight (heart, liver and kidneys) and body composition (amount of epididymal and subcutaneous fat mass) were measured. The tissues collected were either frozen in liquid nitrogen and stored at -80°C or fixed in 4% Paraformaldehyde (PFA) solution and stored in an eluted fixation solution (0.4 % PFA in 100 mmol/L (M) Sodium Phosphate buffer (NaPi)) at 4°C.

All mice were euthanatized and all tissues collected before this master project was initiated. In this master thesis, visceral adipose tissue (epididymal and gonadal fat) and liver tissues have been analysed.

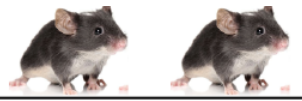
2.2 Methods

2.2.1 Animal experiments

All animal use was approved and registered by the Norwegian Animal Research Authority. In this master thesis, 48 *Plin4*^{+/+} mice and 47 *Plin4*^{-/-} mice in total have been included in three different independent studies. The mice were divided into groups of eight (except for one group of seven mice), where *Plin4*^{+/+} mice and *Plin4*^{-/-} mice, matched with age and gender, were exposed to custom-made diets (Research Diets Inc, USA) (overview in table 5).

The mice included in this study received either of the following diet interventions:

1. Normal access to low fat control diet or the high-fat diet for 10 weeks, from the age of 8 weeks to ~18 weeks
2. Normal access to Western control diet or the Western diet (high in fat/cholesterol/sucrose diet) for 10 weeks, from the age of 8 weeks to ~18 weeks
3. Normal access to standard rodent chow diet or 24 hour fasting at 15 weeks of age



	Diet composition, calories in %			Sample size	
	Carbohydrate	Fat	Protein	<i>Plin4</i> ^{+/+}	<i>Plin4</i> ^{-/-}
High-fat diet	20	60	20	8	8
Low fat control diet	70	10	20	8	8
Western diet	40	40	20	8	8
Western control diet	60	20	20	8	8
Chow diet	58	18	24	8	8
Fasting	-	-	-	8	7

Table 5. Diet compositions and mice included in this study. Mice have been exposed to two separate diet interventions, high-fat diet and Western diet, along with corresponding control diets. Fasted conditions have been investigated in a third intervention, using food deprivation for 24 hours compared to a fed state, where the mice were given free access to chow diet. 48 *Plin4*^{+/+} mice and 48 *Plin4*^{-/-} mice have been included and exposed to different diets. One mouse in the fasting *Plin4*^{-/-} group was excluded based on detection of *Plin4* mRNA, confirming a genotyping error for this mouse. mRNA: messenger ribonucleic acid.

2.2.2 Quantitative reverse transcription polymerase chain reaction

Quantitative reverse transcription polymerase chain reaction (RT-qPCR) was chosen for gene expression analyses. In this procedure, ribonucleic acid (RNA) was isolated, followed by reverse transcription of complementary deoxyribonucleic acid (cDNA).

Tissue homogenisation and RNA isolation

Tissue pieces were homogenised in RA1 buffer containing 1% β -mercaptoethanol (3,5 μ l β -mercaptoethanol in 350 μ l RA1 buffer) for 2 x 30 s/ 5000 rpm in a PreLys24 homogenizer (Bertin instruments).

Sample (mouse)	Amount of tissue	ml RA1 buffer per sample	Beads	(rpm x seconds) x 2
Liver	Tiny pieces / ~5 mg	0,35	Glass	(5000 x 30) x 2
Adipose tissue	Small pieces / ~15 mg	0,35	Glass	(5000 x 30) x 2

Table 6. Tissue homogenisation for RNA isolation. Liver and adipose tissue pieces have been collected and homogenisation in a PreLys24 homogeniser (Bertin instruments). Tissue pieces were homogenised in RA1 buffer containing 1% β -mercaptoethanol (3,5 μ l β -mercaptoethanol in 350 μ l RA1 buffer) with glass pellets as beads. rpm: revolutions per minute.

Total RNA was isolated from adipose tissue and liver homogenate with a NucleoSpin RNA kit (Macherey-Nagel, Düren, Germany) with minor modifications prior to application to the purification column. 350 μ l Phenol:Chloroform:Isoamylalcohol was added to each sample in a fume hood, and the samples were subsequently mixed by shaking the tubes for 20 seconds. All samples were left in room temperature for 5 minutes for the reaction to happen. After 5 minutes waiting, the samples were centrifuged at 9000 revolutions per minute (RPM) for another 5 minutes. Extraction of RNA was performed in a fume hood, and 350 μ l supernatant from each sample were carefully transferred to new Eppendorf tubes. 95 μ l high salt buffer (recipe in table 7) was added to each sample and the samples were subsequently mixed thoroughly by hand. 260 μ l 96 % ethanol (EtOH) was added, and the samples were mixed again. Total sample volume (~700 μ l) were transferred to Nucleospin purification columns for the additional extraction steps.

Components	Stock volume (ml)
NaCl	3,0
Na-Acetate (pH 5,5)	2,67
PCR H ₂ O	4,33
Total volume	10 ml

Table 7. Recipe, high salt buffer. NaCl: Sodium Chloride; Na: Sodium; PCR: polymerase chain reaction; H₂O: water.

Determination of RNA concentration

RNA concentration and quality was determined by measuring absorbance using a Nano Drop ND-1000 spectrophotometer (Thermo Scientific, Waltham, MA) following a previously described protocol (82). RNA concentration was estimated based on the absorption at 260nm, while RNA quality was evaluated based on 230 nm/260 nm and 280 nm/260 nm absorption ratios.

Synthesis of cDNA

Total RNA was reverse-transcribed with multiscribe reverse transcriptase (RT) enzyme into first strand cDNA using random primers, following a protocol described in the High Capacity cDNA Reverse Transcription Kit (Applied Biosystems), similar to the protocol of Haddan *et al.* (83). The recipe for the RT master-mixture is found in table 8.

Reagents	Volume in each tube (µL)	Function of reagent
RNase free H ₂ O	4,2	Diluent
10X RT-buffer	2,0	pH regulation
10X Random Primers	2,0	Primers for cDNA synthesis
dNTP mix	0,8	Building blocks
Multiscribe RT enzyme	1,0	Conversion of mRNA to single stranded cDNA
Total volume	10,0	

Table 8. Recipe, reverse transcriptase master-mix. RT: reverse transcriptase; dNTP: deoxynucleoside triphosphate; cDNA: complementary deoxyribonucleic acid.

Based on the concentrations of each RNA sample and the required amount of RNA in cDNA synthesis, the volume of RNA sample and volume of RNase free H₂O were calculated in a pre-coded Excel sheet. 10 µl of master mix and 10 µl diluted RNA sample made a total of 20 µl reaction volume.

A Mastercycler Ep Gradient S (Eppendorf AG (Hamburg, Tyskland)) was used for cDNA synthesis with these settings:

- Annealing: 10 minutes, 25°C (primers bind to RNA)
- Revers Transcription: 120 minutes, 37°C (RT transcribe complementary DNA (cDNA) with RNA as template)
- Enzyme Inactivation: 5 minutes, 85°C (RT is inactivated at high temperatures)

Each cDNA library was diluted with RNase free H₂O to achieve accurate pipetting in the RT-qPCR analysis. The cDNA libraries were diluted to make a common final cDNA concentration of 5 ng/μl.

Quantitative PCR

qPCR amplifications were performed with intercalating dyes (SYBRGreen, SsoAdvanced, Bio-Rad). Reactions were pipetted into 96 well plates with a final volume of 10 μl, of which 2,5 μl was cDNA and 7,5 μl was master-mix. Master-mix with specific primer pairs (appendix 1) was made for each gene assay (recipe in table 9). SYBRGreen was used as fluorescent dye to detect the amount of double stranded DNA (amplified PCR product). Two controls were run for each primer sample set. The “no-RT” control, lacking the reverse transcriptase enzyme, was performed to confirm absence of DNA contamination and the “no template control” was performed to confirm lack of contamination.

Components	Reagent volume in each well (μl)
SYBRgreen	5,0
PCR H ₂ O	2,3
5' primer (10 μM)	0,1
3' primer (10 μM)	0,1
Total volume	7,5

Table 9. Recipe, master-mix for RT-qPCR. SYBRgreen was used as fluorescent dye to detect the amount of double stranded DNA (amplified PCR product). Specific primer pairs (5' and 3') were used for each gene investigated (appendix 1). PCR: polymerase chain reaction.

A CFX96 Real-Time System Thermal Cycler (Bio-Rad Laboratories (Hercules, CA, US)) and SDS 2.3 software (Applied Biosystems) was used for qPCR amplifications. The cyclic conditions included an initial denaturation step of 3 minutes at 95°C, followed by 40

repetitions of 10 seconds at 95°C and 20 seconds at 60°C. The fluorescence was detected at the end of each cycle.

The comparative $\Delta\Delta\text{CT}$ model (84, 85) was used to quantify the relative mRNA levels of expressed gene. The TATA binding protein (TBP) was used as reference gene in liver and adipose tissue samples (86). The TBP signal was verified to not differ in expression among groups or treatments.

2.2.3 Measuring hepatic content of triacylglycerol and total cholesterol

Quantitative hepatic lipid analysis was performed using colorimetric enzymatic detection kits to measure content of TAG (Triglycerides Enzymatique PAP150, Biomerieux) and total cholesterol (Cholesterol 1600, ERBA Diagnostics, MaxMat) in homogenate of liver tissue. A sample piece of ~20 mg liver tissue was homogenised for 2 x (30 s x 5000 rpm) in a PreLys24 homogenizer in 400 μl phosphate-buffered saline (PBS). After preparation of homogenate, the samples were normalised according to each sample weight and adjusted to a final concentration of 50 mg liver/mL (20 mg liver / 0,4 ml PBS). Homogenates were stored at -80°C until measurements.

Samples were thawed on ice and sonicated to make the samples fully dissolved before measurement of lipid content. 2,5 μl sample (numbered samples in duplicates), blind sample and standard were added to specific wells in a 96 well plate. PBS was used as blind sample and specific standards were used for measuring TAG and cholesterol content. As a final step, 250 μl reconstituted Reagent 3 was added to each well with sample, blind sample and standard, before incubation on the benchtop for 10 minutes (up to 30 minutes).

The 96 well plates were read in a BioTek Synergy H1 microplate reader (BioTek Instruments) at 505 nm absorbance. The content of TAG and total cholesterol were calculated according to the manufactures protocols.

2.2.4 Histological examination

To be able to visualise individual LDs in a tissue, the tissues of interest must be cut in thin sections, stained and mounted on microscopic slides prior to visualisation with a microscopic technique.

Dehydration

Liver tissue pieces fixed with 4% PFA solution and stored in an eluted fixation solution at 4°C (0.4 % PFA in 100 mmol/L (M) NaPi) were used for histological examination. Direct freezing of fresh tissue in liquid nitrogen, on dry ice or in a freezer creates tissue crystals that break down cell membranes and destroy LDs. To avoid tissue destruction when the tissue pieces were frozen, water was removed from the tissues. By step-wise incubation of the liver pieces in sucrose, the water in the tissue was substituted with sucrose, and tissue destruction prevented. 10, 20 and 30 % sucrose solutions containing 0.1 M NaPi were prepared. Squared liver pieces (1 cm in length) were incubated in 5 ml 10 % sucrose at 4°C for one hour. After one hour, 10 % sucrose was removed and 5 ml of 20 % sucrose was added. The liver pieces were incubated for another hour. Finally, 20 % sucrose was removed and 30 % sucrose added. The liver pieces were incubated at 4°C overnight.

Embedding

After incubation of the liver pieces in 30 % sucrose overnight, the liver pieces were transferred into 50 % Optimal Cutting Temperature (OCT) wash solution (100 % OCT diluted with 0,1 M NaPi) for about 1 minute, and then into 100 % OCT for another minute. Each liver piece was then transferred into a well in the embedding tray and submerged in 100 % OCT. The embedding tray with liver pieces in 100 % OCT were then transferred to a Styrofoam box filled with liquid nitrogen and allowed to freeze in liquid nitrogen vapour. When the OCT had turned white as a sign of the liver pieces being frozen, the embedding tray was transferred to a refrigeration device called a cryostat (-20°C) for the mould to thaw/soften. When the embedding tray was soft enough for the embedded liver pieces to be bent out, the moulded blocks were transferred to an Eppendorf tube filled with a small piece of tissue paper in the bottom. The paper was added to avoid the moulded blocks to stick to the bottom of the tube. The tubes were stored at -80°C.

Sectioning

Sectioning of the OCT embedded liver pieces were carried out in the cryostat. Sections of 20 μm were cut at -20°C . The cut sections were carefully transferred to a 12 well plate, containing 1,5-1,8 ml cryoprotection solution for sections (recipe in table 10). Pending for staining, parafilm was put between the lid and the plate, and the sections were stored at 4°C for a few hours or at -20°C for long term storage.

Components	Reagents volume in each well
Sucrose	150 g
PVP-40	5 g
Ethylene glycol	150 ml
0,1 M NaPi	~350 ml
Total volume	500 ml

Table 10. Recipe, cryoprotection solution. PVP-40 was added to 250 ml 0,1 M NaPi and stirred to dissolve. Sucrose was slowly added to dissolve, and the ethylene glycol was added subsequently. The final volume was brought to 500 ml by adding additional 0,1 M NaPi (~100 ml 0,1 M NaPi). PVP-40: Polyvinyl-pyrrolidone; NaPi: Sodium Phosphate buffer.

Tissue staining

The sections were carefully transferred to a new 12 well plate containing 1,6 ml 0,1 M NaPi (containing 0.02 % sodium azide (NaN_3)) in each well. NaN_3 was added to prevent bacteria growth if the sections were stored for more than 2 days (up to 1 week). Sections were washed twice with 0,1 M NaPi (containing 0,02 % NaN_3) to remove the cryoprotection solution. Before staining, the 0,1 M NaPi was removed, and each well was added 800 μL staining solution containing Bodipy, Phalloidin-CF568 conjugate and Hoechst, mixed in 0,1 M NaPi (recipe in table 11). Staining was performed according to the protocol describes in Pratt *et. al.* (87), except for one modification. Instead of staining sequentially, liver sections were stained simultaneously with a mixture of three stains in 0,1 M NaPi. The sections were incubated with staining solution at room temperature for 25 minutes.

		Property
Bodipy (B) 1 mM stock	Dilute 1:1000	Green fluorescence dye that stain neutral lipids within the LDs
Phalloidin-CF568 conjugate (P) 200 U/MI stock	Dilute 1:200	Phalloidin is a toxin from mushroom with a high affinity for F-actin. CF568 is a fluorescence dye that gives out a red signal. The conjugation of these two will show the F-actin of the cells, which are rich in cell membranes
Hoechst (H) 20 mM stock	Dilute 1:4000	Blue fluorescence dye that stain DNA (nuclei) by binding to ds-DNA

Table 11. Staining solution. The staining solution was made in the dark to prevent ruining the dyes. 30 ml 0,1 M NaPi was added 30 µl Bodipy, 150 µl Phalloidin CF568 conjugate and 7,5 µl Hoechst. DNA: deoxyribonucleic acid; ds: double stranded; LD: lipid droplet.

After staining, the sections were washed twice with 1,6 ml 0,1 M NaPi to remove the staining solution, before being mounted to microscopic slides. 100 µl NaPi was added to each slide. The sections were transferred with a wet pencil brush before the NaPi was removed with a pipette (the sections should not be touched). When the sections had dried slightly, the slides were mounted in mounting media (ProLong® Diamond Antifade Mountant, Thermo Fisher Scientific), covered with coverslips and left in room temperature overnight for the mounting media to become solid. The slides were scanned under a 20 x objective with an Axio Scan Z1 system (Zeiss). The digital images were analysed in Zen 2.3 imaging software (blue edition). Images with the most representative morphology and staining were manually evaluated and chosen to demonstrate the results. The slides were stored long term at -20°C.

2.2.5 Statistical methods

All data are presented as Means \pm standard error of the mean (SEM). Significant differences between more than two independent groups were evaluated by one-way analysis of variance (ANOVA). Bonferroni's Multiple Comparison test was chosen as post hoc test to assess significance between the groups. Barlett's test for homogeneity of variances were used to determine equal variances between the samples. Welch's unequal variances t-test was used to evaluate the difference between two independent groups. A P-value $< 0,05$ was considered statistically significant. All statistical analyses were performed in GraphPad Prism Software (La Jolla, CA).

3 Results

This master thesis has investigated the role of *Plin4* in adipose tissue and liver under fed and fasted conditions by comparing *Plin4*^{+/+} and *Plin4*^{-/-} mice. Mice have been exposed to two separate diet interventions, high-fat diet and Western diet, along with corresponding control diets. Fasted conditions have been investigated in a third intervention, using food deprivation for 24 hours compared to a fed state, where the mice were given free access to chow food. At the end of the interventions, animals and dissected tissues were weighted and collected, respectively, for molecular analyses. In this master thesis, molecular analyses consist of gene expression, LD morphology, and content of TAG and total cholesterol in liver and adipose tissue.

3.1 High-fat diet intervention

Plin4 is expressed in high levels in adipose tissue (75), which suggests that *Plin4* might be important for LD storage in this tissue. We therefore exposed *Plin4*^{+/+} and *Plin4*^{-/-} mice to a low-fat control diet (10 E% fat, 70E% carbohydrates and 20 E% protein) or a high-fat diet (60 E% fat, 20 E% carbohydrates and 20 E% protein). Similar high-fat diets have been used previously to induce insulin resistance and fatty liver in mice (72).

3.1.1 Mice characteristics

The intervention included 16 *Plin4*^{+/+} and 16 *Plin4*^{-/-} male mice. Eight mice of each genotype were fed either the low-fat control diet or the high-fat diet for ~10 weeks, from 8 weeks of age until 18 weeks of age. As expected, there were a significant increase in body weight in mice that had received the high-fat diet compared to the mice receiving control diet in both *Plin4*^{+/+} and *Plin4*^{-/-} mice (table 12). The increase in body weight were largely attributed to by expansion of adipose tissues, as there was a significant increase in the amount of epididymal and subcutaneous fat depots in the high-fat diet groups, and no differences in the weight of other central organs (heart, liver, kidneys). No significant differences were detected in animal weights or organ weights between *Plin4*^{+/+} and the *Plin4*^{-/-} mice receiving the same diet.

KTD-M96 Male mice	WT-CD	KO-CD	WT-HFD	KO-HFD
Body weight (g)	33,5 ± 1,2	33,3 ± 1,2	41,6 ± 1,2***	40,6 ± 1,5***
Heart (gm)	0,137 ± 0,007	0,132 ± 0,004	0,129 ± 0,003	0,125 ± 0,002
Liver (gm)	1,55 ± 0,06	1,58 ± 0,10	1,62 ± 0,06	1,56 ± 0,09
Kidneys (gm)	0,32 ± 0,02	0,35 ± 0,01	0,36 ± 0,01	0,36 ± 0,01
EPI fat (gm)	0,82 ± 0,18	0,83 ± 0,10	2,33 ± 0,15***	2,27 ± 0,10***
SUB fat (gm)	0,47 ± 0,10	0,50 ± 0,07	1,30 ± 0,16***	1,28 ± 0,13***

Table 12. Mice characteristics after ~10 weeks of a high-fat diet intervention. The intervention included 16 *Plin4*^{+/+} and 16 *Plin4*^{-/-} male mice. Eight mice of each genotype were fed either the low-fat control diet or the high-fat diet for ~10 weeks, from 8 weeks of age until 18 weeks of age. At the end of the interventions, animals and dissected tissues were weighted and collected for molecular analyses. Data are shown as Means ± SEM (n = 8 mice per group). Statistical significance were determined by Bonferroni's multiple comparison test (*p < 0,05; **p < 0,01; ***p < 0,001). WT: *Plin4*^{+/+} (wild-type); KO: *Plin4*^{-/-} (knock-out); CD: control diet (low-fat control diet); HFD: high-fat diet; SEM: standard error of the mean.

3.1.2 Gene expression analysis

Absence of a gene may result in compensatory responses through upregulation of genes with similar function. We therefore investigated whether absence of *Plin4* affected gene expression of Plin family members as well as genes involved in lipid metabolism. We focused our gene expression analyses on epididymal fat and liver, and compared expression between *Plin4*^{+/+} and *Plin4*^{-/-} mice receiving the low-fat control diet or the high-fat diet.

Epididymal fat

We first measured gene expression of all five Plin mRNAs in epididymal fat by RT-qPCR. As expected, the mRNA levels of *Plin4* was highly expressed in *Plin4*^{+/+} mice, but completely absent in the *Plin4*^{-/-} mice (figure 1 D). There were no difference in the mRNA levels of *Plin1*, *Plin2* and *Plin3* in the absence of *Plin4* (figure 1 A, B and C). No change in expression levels were seen in *Plin1* and *Plin3* between mice receiving high-fat diet compared to low-fat control diet, while the expression of *Plin2* increased significantly in mice receiving the high-fat diet (figure 1 B). The gene expression of *Plin5* were significantly increased in *Plin4*^{-/-} mice receiving high-fat diet compared to *Plin4*^{+/+} mice (figure 1 E). In sum, expression of Plin family members were relatively unaffected by the removal of *Plin4*.

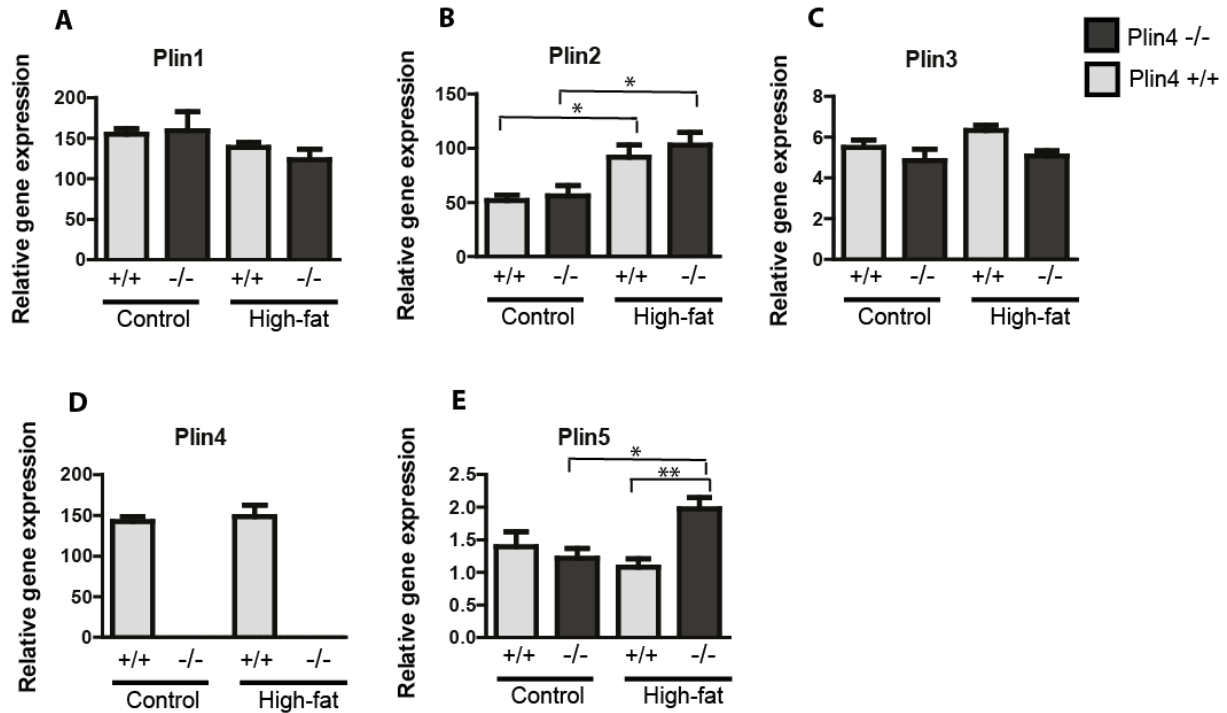


Figure 1. Gene expression of Plin family members, epididymal fat, high-fat diet intervention. The intervention included 16 *Plin4*^{+/+} and 16 *Plin4*^{-/-} male mice. Eight mice of each genotype were fed either the low-fat control diet or the high-fat diet for ~10 weeks, from 8 weeks of age until 18 weeks of age. Gene expression of Plin family members in epididymal fat were analysed with RT-qPCR, related to the expression of TBP. Data are shown as Means \pm SEM (n = 8 mice in each group). Statistical significance was determined by Bonferroni's multiple comparison test (*p < 0,05; **p < 0,01; ***p < 0,001). RT-qPCR: quantitative reverse transcription polymerase chain reaction; TBP: TATA binding protein; SEM: standard error of the mean.

We next investigated the gene expression of *PPAR α* and *PPAR γ* , two fatty acid-sensing transcription factors expressed in adipose tissue. Gene expression of both *PPAR α* and *PPAR γ* were significantly reduced in mice receiving the high-fat diet compared to mice receiving the low-fat control diet (p < 0,05 for both *Plin4*^{-/-} and *Plin4*^{+/+} mice), but no changes were seen between the *Plin4*^{-/-} and *Plin4*^{+/+} mice (data not shown). Due to a lack of changes in adipose tissue weight or expression of key adipogenic genes in the absence of *Plin4*, we concluded that lack of *Plin4* likely does not result in large changes in gene expression in mice adipose tissue. To further investigate the role of *Plin4* in mice on a high-fat diet, we therefore focused our analysis on liver.

Liver tissue

Gene expression of *Plin4* increased several fold in the *Plin4*^{+/+} mice on high-fat diet compared to the low-fat control diet (figure 2 D), whereas no expression was detected in the livers of *Plin4*^{-/-} mice. The mRNA levels of *Plin5* was significantly lower in *Plin4*^{-/-} mice compared to *Plin4*^{+/+} mice on the high-fat diet (figure 2 E), and there were a tendency of lower *Plin5* expression in *Plin4*^{-/-} mice receiving the low-fat control diet. There were also a tendency of reduced mRNA level of *Plin3* in *Plin4*^{-/-} mice on a high-fat diet, although non-significant. Expression of *Plin1* and *Plin2* were unaffected by the removal of *Plin4*. In sum, expression of Plin family members were relatively unaffected by the absence of *Plin4*, which argues against a transcriptional compensation in expression of Plin family members.

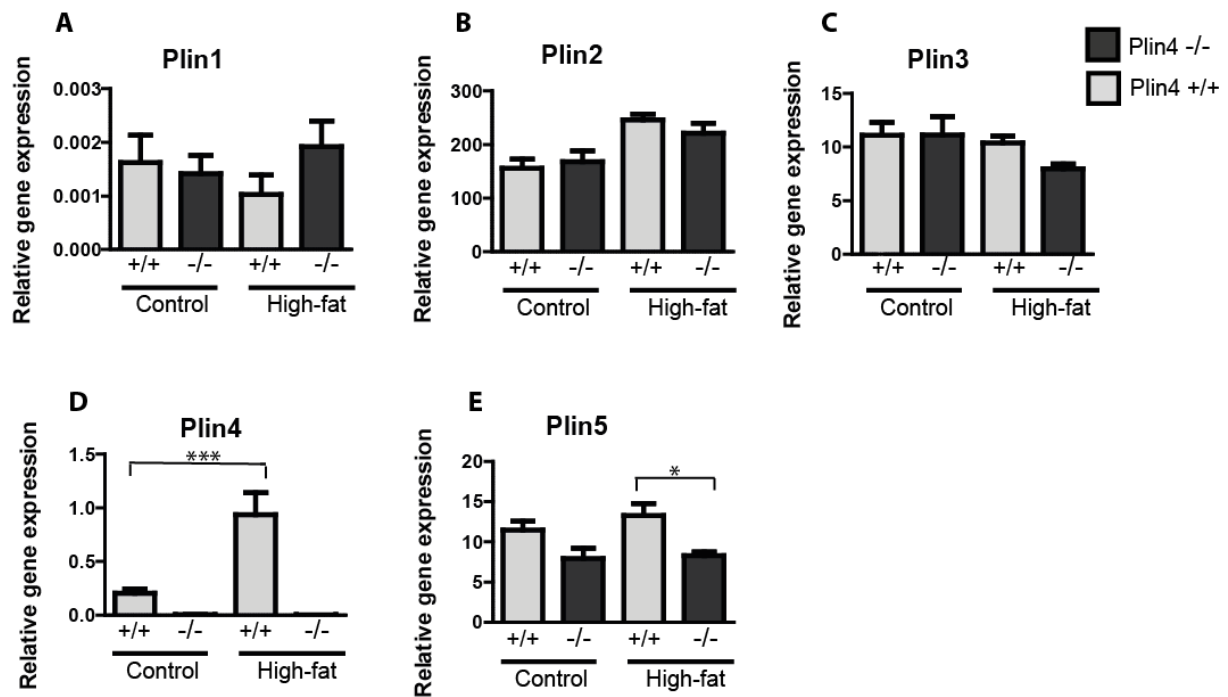


Figure 2. Hepatic gene expression of Plin family members, high-fat diet intervention. The intervention included 16 *Plin4*^{+/+} and 16 *Plin4*^{-/-} male mice. Eight mice of each genotype were fed either the low-fat control diet or the high-fat diet for ~10 weeks, from 8 weeks of age until 18 weeks of age. Gene expression of Plin family members in liver were analysed with RT-qPCR, related to the expression of TBP. Data are shown as Means ± SEM (n = 8 mice in each group). Statistical significance was determined by Bonferroni's multiple comparison test (*p < 0,05; **p < 0,01; ***p < 0,001). RT-qPCR: quantitative reverse transcription polymerase chain reaction; TBP: TATA binding protein; SEM: standard error of the mean.

We next investigated gene expression of PPARs. The mRNA levels of *Ppara* and *Pparγ* were significantly increased in both genotypes on a high-fat diet compared to the low-fat control diet (data not shown), but no difference were seen between the two genotypes.

Based on these initial analyses, where absence of *Plin4* does not affect body weight, organ weight or gene expression amongst Plin family members and *Ppars* in adipose tissue and liver (except for gene expression of *Plin5*), we concluded that absence of *Plin4* likely not affect the response to a high-fat diet. To search for a functional role of *Plin4*, we therefore decided to investigate if the absence of *Plin4* could affect gene expression in mice receiving an energy dense diet with elevated levels of fatty acids, cholesterol and carbohydrates, termed a Western diet.

3.2 Western diet intervention

Plin4^{+/+} and *Plin4*^{-/-} mice were exposed to a Western control diet (composed of 20 E% fat, 0,1 % w/w cholesterol, 60 E% carbohydrates and 20 E% proteins) or the Western diet (composed of 40 E% fat, 1 % w/w cholesterol, 40 E% carbohydrates and 20 E% proteins). The Western diet is characterised by high levels of sugar and fat, and low intake of fibre and vegetables, with a following increased risk for chronic diseases (88).

3.2.1 Mice characteristics

The intervention included 16 *Plin4*^{+/+} and 16 *Plin4*^{-/-} female mice. Eight mice of each genotype were fed either a Western control diet or the Western diet for ~10 weeks, from 8 weeks of age until 18 weeks of age. As expected, there were an increase in body weight in mice receiving Western diet compared to mice receiving Western control diet (table 13). The increase was only significant in the *Plin4*^{-/-} mice, but same tendency was also seen in the *Plin4*^{+/+} mice. There were found an increase in fat mass between the two diet groups, although non-significant. We observed significant increase in liver size in both *Plin4*^{+/+} and *Plin4*^{-/-} mice on the Western diet compared to the Western control diet. No differences were detected in animal weight or organ weights between *Plin4*^{+/+} and *Plin4*^{-/-} mice receiving the same diets.

KTD-M95 Female mice	WT-CD	KO-CD	WT-WD	KO-WD
Body weight (g)	26,0 ± 1,8	24,5 ± 1,2	29,9 ± 1,2	30,7 ± 0,8*
Heart (gm)	0,097 ± 0,002	0,095 ± 0,003	0,105 ± 0,005	0,103 ± 0,002
Liver (gm)	098 ± 0,09	0,85 ± 0,04	1,38 ± 0,08***	1,38 ± 0,04***
Kidneys (gm)	0,221 ± 0,004	0,223 ± 0,008	0,249 ± 0,012	0,247 ± 0,005
EPI fat (gm)	0,83 ± 0,21	0,70 ± 0,12	1,14 ± 0,19	1,219 ± 0,11
SUB fat (gm)	0,54 ± 0,14	0,47 ± 0,08	0,69 ± 0,09	0,77 ± 0,08

Table 13. Mice characteristics after ~10 weeks of a western diet intervention. The intervention included 16 *Plin4*^{+/+} and 16 *Plin4*^{-/-} female mice. Eight mice of each genotype were fed either a Western control diet or the Western diet for ~10 weeks, from 8 weeks of age until 18 weeks of age. At the end of the interventions, animals and dissected tissues were weighted and collected for molecular analyses. Data are shown as Means ± SEM (n = 8 mice per group). Statistical significance were determined by Bonferroni's multiple comparison test (*p < 0,05; **p < 0,01; ***p < 0,001). WT: wild-type (*Plin4*^{+/+}); KO: knock-out (*Plin4*^{-/-}); CD: control diet (western control diet); WD: western diet; SEM: standard error of the mean.

3.2.2 Gene expression analysis

Absence of a gene may results in compensatory responses through upregulation of genes with similar function. We therefore investigated whether absence of *Plin4* affected gene expression of Plin family members as well as other genes involved in lipid metabolism by RT-qPCR. We focused our gene expression analyses on gonadal fat and liver, and compared the expression between *Plin4*^{+/+} and *Plin4*^{-/-} mice receiving a Western control diet or the Western diet.

Gonadal fat

We first measured gene expression of all five Plin family members in gonadal fat. As expected, the mRNA levels of *Plin4* was highly expressed in *Plin4*^{+/+} mice, but completely absent in the *Plin4*^{-/-} mice (data not shown). There were no difference in the mRNA levels of *Plin1*, *Plin2*, *Plin3* or *Plin5* in the absence of *Plin4* (data not shown). No significant changes were seen in any of the Plin family members in response to the diet intervention in *Plin4*^{-/-} or *Plin4*^{+/+} mice.

We next investigated the gene expression of *Ppars* and *Lxrs*, and no significant changes were found (data not shown). Based on the lack of effect of *Plin4* ablation on gene expression in gonadal fat, we concluded that the absence of *Plin4* likely does not result in large gene expression alterations in adipose tissue in this diet intervention. To further investigate the role of *Plin4* in female mice on the Western diet, we therefore focused our analysis on liver.

Liver tissue

Gene expression of *Plin4* increased several fold in the *Plin4*^{+/+} mice on the Western diet compared to the Western control diet (figure 3 D), whereas no expression was detected in the livers of *Plin4*^{-/-} mice. The mRNA levels of *Plin1* in liver tissue were almost non-detectable, which was expected based on previous tissue expression patterns (38). The mRNA levels of *Plin3* and *Plin5* were significantly lower in the *Plin4*^{-/-} mice compared to *Plin4*^{+/+} mice on the Western control diet (figure 3 C and E respectively). Expression of *Plin1* and *Plin2* was unaffected by the absent of *Plin4*. In sum, expression of Plin family members were unaffected by the removal of *Plin4* in mice receiving Western diet, but some significant differences were seen in mice receiving the Western control diet, a diet low in fat and high in carbohydrates.

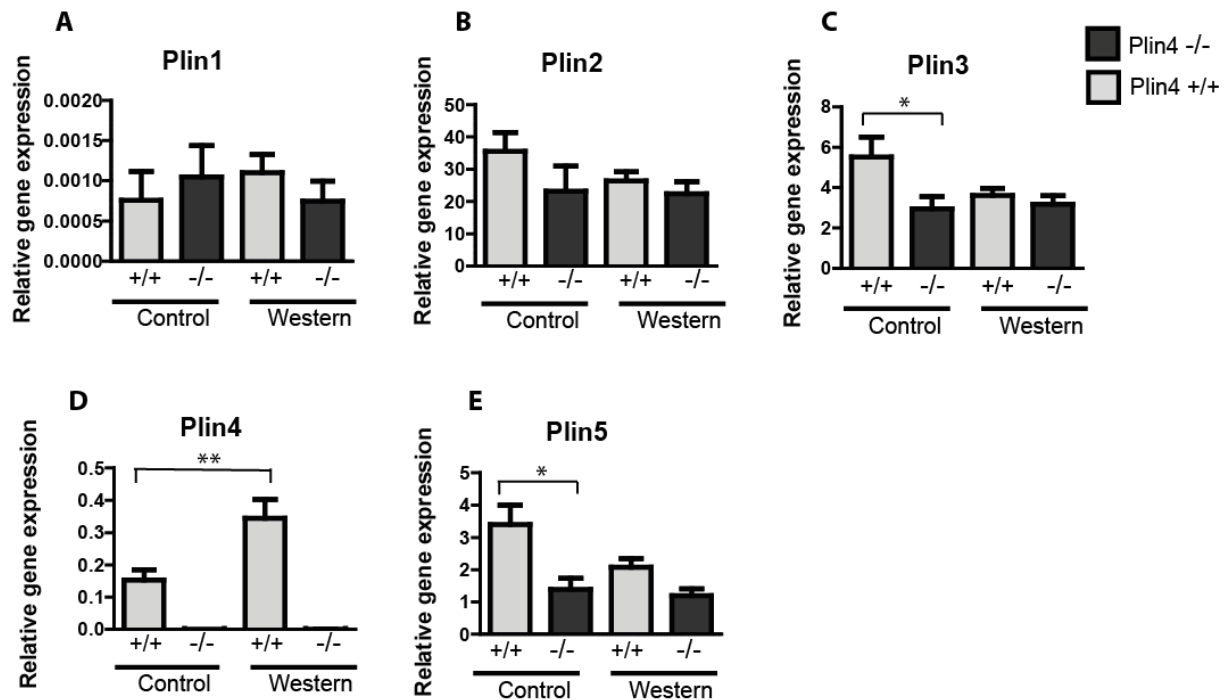


Figure 3. Hepatic gene expression of Plin family members, western diet intervention. The intervention included 16 *Plin4*^{+/+} and 16 *Plin4*^{-/-} female mice. Eight mice of each genotype were fed either a Western control diet or the Western diet for ~10 weeks, from 8 weeks of age until 18 weeks of age. Gene expression of Plin family members in liver were analysed with RT-qPCR, related to the expression of TBP. Data are shown as Means ± SEM (n = 8 mice in each group). Statistical significance was determined by Bonferroni's multiple comparison test (*p < 0,05; **p < 0,01; ***p < 0,001). RT-qPCR: Quantitative reverse transcription polymerase chain reaction; TBP: TATA binding protein; SEM: standard error of the mean.

We next investigated expression of genes involved in the lipid metabolism. We decided to investigate gene expression patterns to a greater degree in this diet intervention, and therefore analysed general lipogenic transcription factors, enzymes involved in lipogenesis and fatty acid synthesis, and enzymes involved in cholesterol uptake and efflux. As expected, mice receiving the Western diet showed lower expression of *Srebp1a* (figure 4 E) and sequentially the target genes of the transcription factor, *Fasn*, *Dgat1* and *Dgat2* (figure 4 H, I and J), enzymes involved in lipogenesis. In *Plin4*^{+/+} mice receiving Western control diet, gene expression of *Srebp1a*, *Fasn*, *Dgat1* and *Dgat2* were correspondingly high, as expected. Unexpectedly, these enzymes were significantly lower in *Plin4*^{-/-} mice receiving the Western control diet compared to *Plin4*^{+/+} mice (figure 4 E, H and I). The gene expression of *Srebp1c* and *Dgat2* were also lower in *Plin4*^{-/-} mice receiving Western control diet, although non-significant (figure 4 F and J).

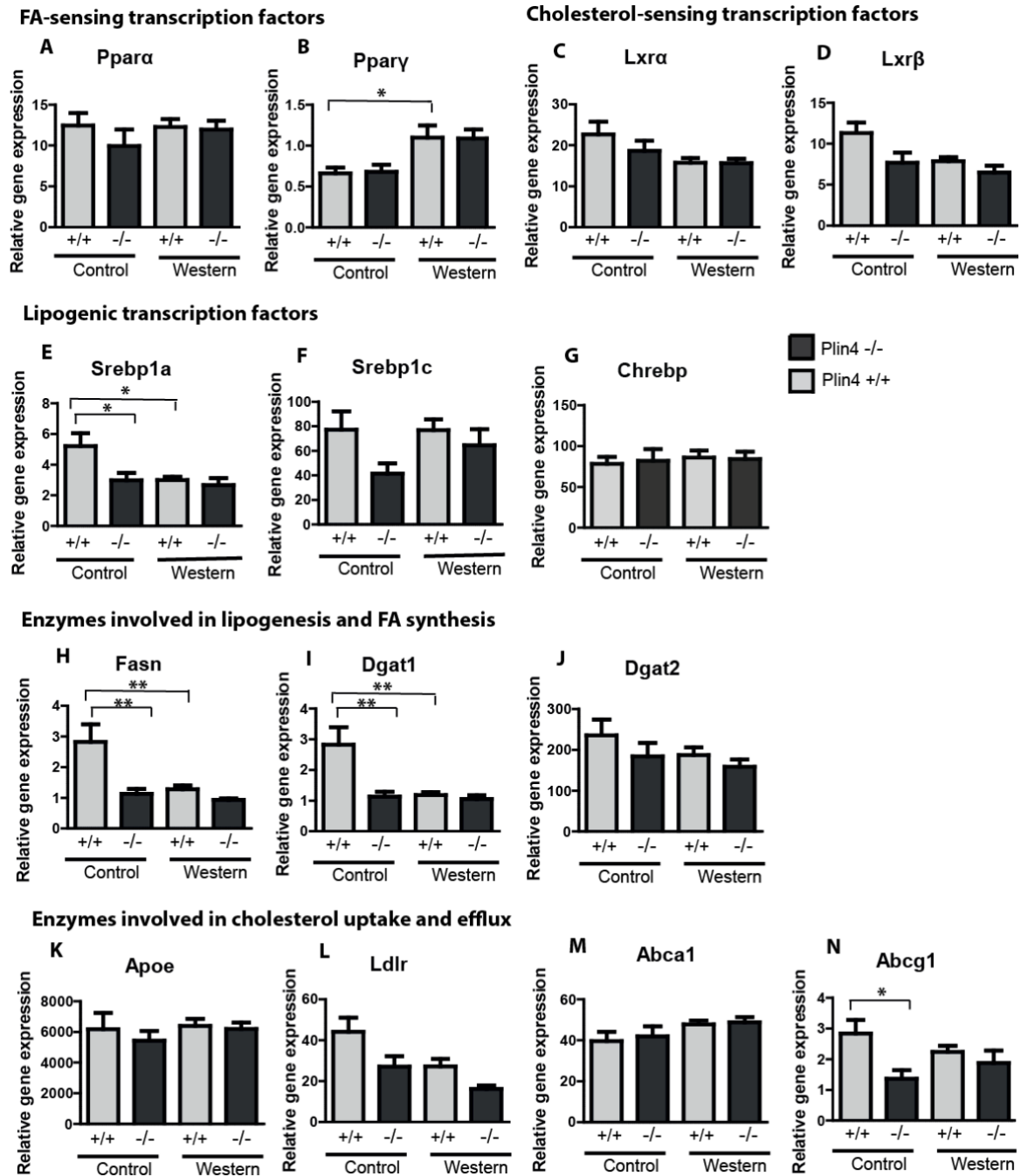


Figure 4. Hepatic expression of genes involved in lipid metabolism, western diet intervention. The intervention included 16 *Plin4*^{+/+} and 16 *Plin4*^{-/-} female mice. Eight mice of each genotype were fed either a Western control diet or the Western diet for ~10 weeks, from 8 weeks of age until 18 weeks of age. Expression of genes involved in lipid metabolism were analysed with RT-qPCR, related to the expression of TBP. Data are shown as Means ± SEM (n = 8 mice in each group). Statistical significance was determined by Bonferroni's multiple comparison test (*p < 0,05; **p < 0,01; ***p < 0,001). RT-qPCR: Quantitative reverse transcription polymerase chain reaction; TBP: TATA binding protein; SEM: standard error of the mean.

Due to significant changes in gene expression of *Srebp1a*, *Fasn* and *Dgat1*, and similar tendency in *Srebp1c* and *Dgat2*, it seems like the rate of lipogenesis in liver may be reduced in *Plin4*^{-/-} mice receiving a diet low in fat and rich in carbohydrates, compared to *Plin4*^{+/+} mice. Based on these results, we wanted to investigate potential changes in hepatic content of lipids between *Plin4*^{+/+} and *Plin4*^{-/-} mice.

3.2.1 Content of triacylglycerol and total cholesterol

Previous studies have shown that the absence of *Plin2* reduces hepatic content of TAG (72). We wanted to investigate if the absence of *Plin4* also reduces hepatic lipid content in mice receiving a Western control diet or the Western diet.

As expected, the difference in dietary factors between Western control diet and Western diet resulted in a significant increase in TAG and total cholesterol in both *Plin4*^{+/+} and *Plin4*^{-/-} mice (figure 5 A and B). These data correspond to the previous observations of increased liver weight (table 13). The amount of TAG and total cholesterol in liver tissue were not significantly different between *Plin4*^{+/+} and *Plin4*^{-/-} mice (figure 5 A and B), and neither were the differences in liver weight (table 13).

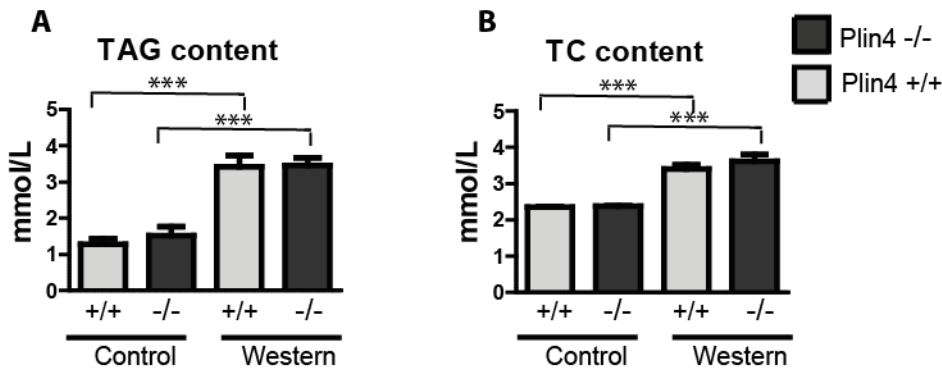


Figure 5. Hepatic content of triacylglycerol and total cholesterol, western diet intervention. The intervention included 16 *Plin4*^{+/+} and 16 *Plin4*^{-/-} female mice. Eight mice of each genotype were fed either a Western control diet or the Western diet for ~10 weeks, from 8 weeks of age until 18 weeks of age. Hepatic lipid content of TAG and total cholesterol were measured using colorimetric kits. Data are shown as Means \pm SEM (n = 8 mice in each group). Statistical significance was determined by Bonferroni's multiple comparison test (*p < 0,05; **p < 0,01; ***p < 0,001). TAG: triacylglycerol; TC: total cholesterol; SEM: standard error of the mean.

No significant differences in liver size or hepatic lipid content were seen between the genotypes, and based on this we have no evidence to suggest that *Plin4* is of decisive importance in hepatic storage of TAG and total cholesterol in mice receiving Western control diet or Western diet, even though significant changes in gene expression were found.

3.2.2 Histology

We next wanted to investigate if changes seen in hepatic lipid content also were protruding in histological examinations. Sections of liver tissue were stained with three different dyes to investigate LD morphology. Bodipy stain neutral lipids green, Phalloidin-CF568 conjugate stain cell membranes red, and Hoechst stain double stranded DNA blue. As expected, increased staining of neutral lipids with Bodipy dye (green colour) were seen in mice receiving Western diet compared to Western control diet. We observed no apparent differences in LD staining between the *Plin4*^{+/+} and *Plin4*^{-/-} mice receiving Western control diet or Western diet (figure 6). This corresponds well to the measurement of hepatic lipid content shown in figure 5 A and B.

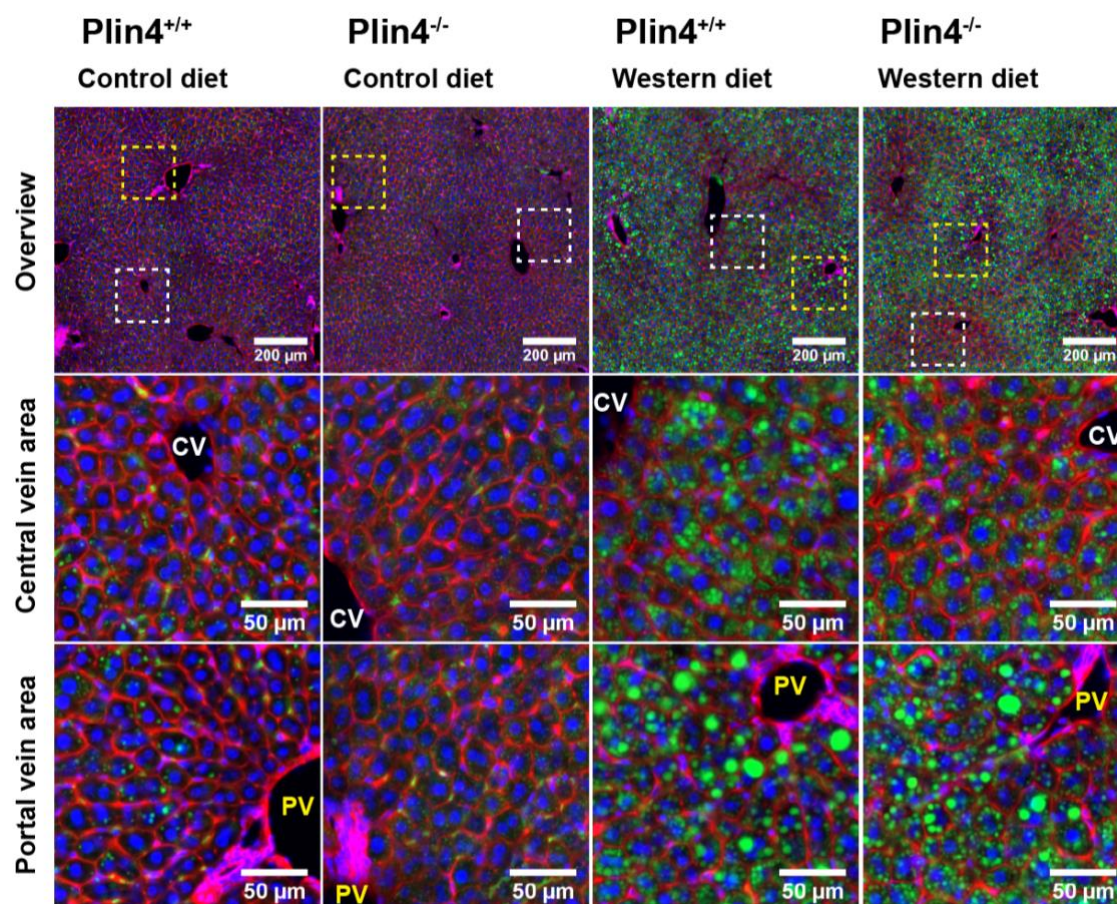


Figure 6. Histological appearance of hepatic lipid content, western diet intervention. The intervention included 16 *Plin4*^{+/+} and 16 *Plin4*^{-/-} female mice. Eight mice of each genotype were fed either a Western control diet or the Western diet for ~10 weeks, from 8 weeks of age until 18 weeks of age. OCT was used as embedding medium, and the liver tissue sections were stained with Bodipy, Phalloidin-CF568 conjugate and Hoechst. Bodipy stain neutral lipids green, Phalloidin-CF568 conjugate stain cell membranes red, and Hoechst stain double stranded DNA blue. The sections were scanned under a 20 x objective with an Axio Scan Z1 system (Zeiss). The digital images were analysed in Zen 2.3 imaging software (blue edition). Images with the most representative morphology and staining were manually evaluated and chosen to demonstrate the results. CV: central vein; PV: portal vein; OCT: optimal cutting temperature.

Based on these results there are no clear evidence that suggest that the *Plin4* has a decisive role in lipid metabolism in mice receiving Western control diet or Western diet. To search for a functional role for *Plin4*, we therefore decided to investigate if the absence of *Plin4* could affect gene expression in the lack of nutrient supply (fasting mice).

3.3 Fasting

After intake of a carbohydrate rich diet, insulin is elevated and glucose predominates as the primary energy source (89). Insulin represses lipolysis in adipose tissue and the flow of fatty acids goes from the liver to the adipose tissue for storage (89). The transition from fed to fasted results in a fall in insulin concentration and increased lipolysis in adipose tissue. The lipolytic degradation of TAG in adipocyte storages releases NEFAs and glycerol to the circulation. Fatty acids are used as energy source for different tissues, while glycerol is used for generation of glucose through hepatic gluconeogenesis (22). The hepatic lipid content increases temporary during fasting due to re-esterification of fatty acids to TAG in the hepatocytes (89).

3.3.1 Mice characteristics

The fasting intervention included 16 *Plin4*^{+/+} and 15 *Plin4*^{-/-} male mice. Originally, there were 16 mice in the *Plin4*^{-/-} group as well, but after RT-qPCR there were found presence of *Plin4* mRNA, and the mice were therefore removed from the *Plin4*^{-/-} group. All of the mice were given chow diet, but eight *Plin4*^{+/+} mice and seven *Plin4*^{-/-} mice were fasted for 24 hours by food deprivation. As expected, there were seen a reduction in body weight in fasted mice compared to mice receiving chow diet. The reduction in body weight were significant in *Plin4*^{-/-} mice (table 14). Liver weight was reduced in both *Plin4*^{+/+} and *Plin4*^{-/-} fasting mice compared to mice fed a chow diet, which corresponds to normal physiology and reduced

amount of stored glycogen in response to fasting. No significant differences were found in amount of epididymal and subcutaneous fat between fed and fasted state in neither *Plin4*^{+/+} nor *Plin4*^{-/-} mice.

KTD-M85 Male mice	WT-Fed	KO-Fed	WT-Fast	KO-Fast
Body weight (g)	29,7 ± 0,7	28,0 ± 0,6	26,5 ± 0,9	24,2 ± 0,7*
Heart (gm)	0,120 ± 0,004	0,128 ± 0,003	0,123 ± 0,003	0,123 ± 0,005
Liver (gm)	1,42 ± 0,07	1,35 ± 0,05	1,07 ± 0,02***	1,04 ± 0,05***
Kidneys (gm)	0,34 ± 0,01	0,34 ± 0,02	0,34 ± 0,01	0,31 ± 0,02
EPI fat (gm)	0,59 ± 0,07	0,24 ± 0,02□□	0,43 ± 0,11	0,10 ± 0,02□
SUB fat (gm)	0,35 ± 0,05	0,26 ± 0,11	0,21 ± 0,05	0,06 ± 0,01

Table 14. Mice characteristics in mice receiving chow diet and fasted for 24 hours. The intervention included 16 *Plin4*^{+/+} and 15 *Plin4*^{-/-} male mice. All mice were fed the chow diet until the fasting period. Eight *Plin4*^{+/+} mice and seven *Plin4*^{-/-} mice were fasted by food deprivation for 24 hours at ~15 weeks of age. At the end of the interventions, animals and dissected tissues were weighted and collected for molecular analyses. Data are shown as Means ± SEM (n = 8 mice per group, except *Plin4*^{-/-} -fast: n = 7 mice). Statistical significance was determined by Bonferroni's multiple comparison test (*p < 0,05; **p < 0,01; ***p < 0,001). In this table, □ represent changes between genotypes in the same diet group. WT: *Plin4*^{+/+} (wild-type); KO: *Plin4*^{-/-} (knock-out); SEM: standard error of the mean.

There were although found a difference in amount of epididymal fat between the genotypes. The amount of epididymal fat were reduced several folds in *Plin4*^{-/-} mice compared *Plin4*^{+/+} mice, both under fed and fasted conditions (figure 7 A). No differences were seen in liver weight or any other organ weight between the two genotypes. There was also found a significant difference in loss of body weight in mice fasted for 24 hours (figure 7 B). *Plin4*^{+/+} mice lost on average 4,5 grams ± 0,2 grams during 24 hours fast, while *Plin4*^{-/-} mice lost on average 5,4 grams ± 0,2 grams (p < 0,05).

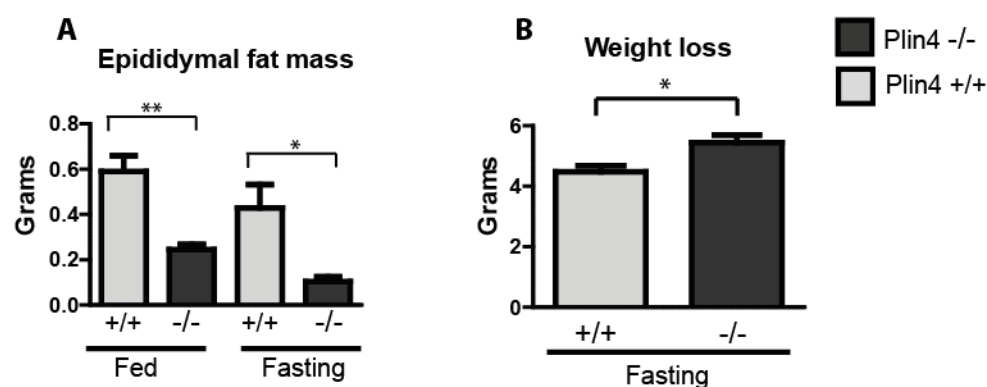


Figure 7. Amount of epididymal fat and weight loss, fasting intervention. The intervention included 16 *Plin4*^{+/+} and 15 *Plin4*^{-/-} male mice. All mice were fed the chow diet until the fasting period. Eight *Plin4*^{+/+} mice and seven *Plin4*^{-/-} mice were fasted by food deprivation for 24 hours at ~15 weeks of age. Epididymal fat mass and body weight have been measured before and after fasting. Data are shown as Means \pm SEM (n = 8 mice per group, except *Plin4*^{-/-} -fast: n = 7 mice). Statistical significance was determined by Bonferroni's multiple comparison test or Welch's unequal variances t-test (*p < 0,05; **p < 0,01; ***p < 0,001).

3.3.2 Gene expression

Based on previous lack of results in adipose tissue in a fed state (seen in this master thesis) liver tissue was chosen for further investigation in the fasting intervention.

The Plins

We investigated the gene expression of all five Plin family members in liver tissue. The mRNA levels of *Plin4* was completely absent in the *Plin4*^{-/-} mice (except for one mouse, which was excluded from the study). The gene expression of *Plin4* in liver increased in response to fasting (figure 8 D), and the same increase was seen in *Plin1*, *Plin2* and *Plin5* in *Plin4*^{+/+} mice (figure 8 A, B and E). This corresponds to increased hepatic lipid content and increased hepatic production of LDs (requiring Plins) in response to fasting (89). Interestingly, the mRNA levels of *Plin5* was significantly lower in fasted *Plin4*^{-/-} mice compared to fasted *Plin4*^{+/+} mice (figure 8 E) and the same tendency was seen for *Plin1* and *Plin2*, although non-significant. This may indicate lower requirement of Plins for hepatic TAG storage in fasted mice lacking *Plin4*.

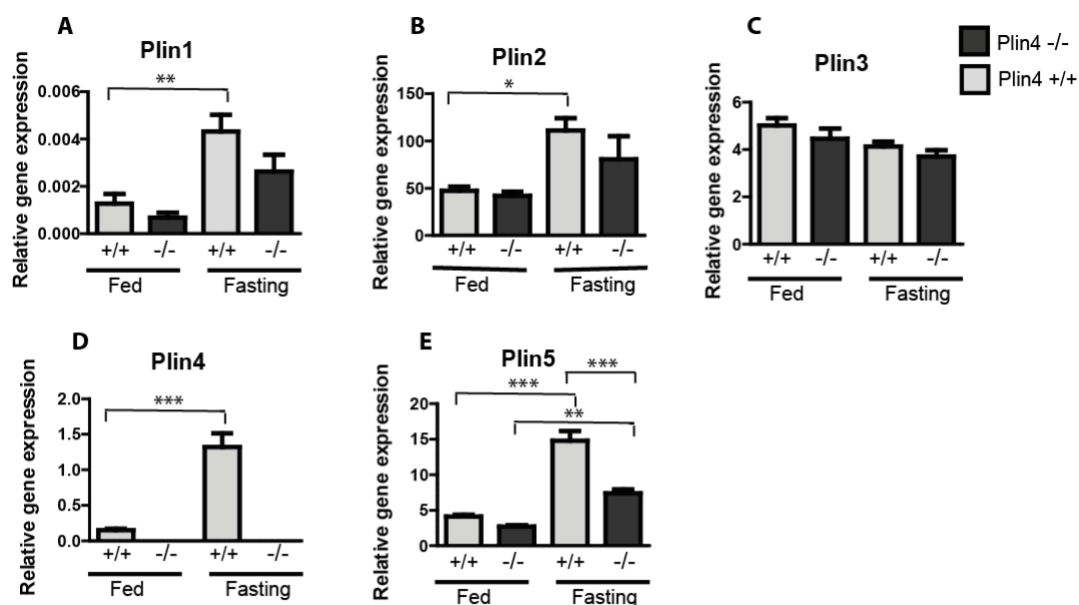


Figure 8. Hepatic gene expression of Plin family members, fasting intervention. The intervention included 16 *Plin4*^{+/+} and 15 *Plin4*^{-/-} male mice. All mice were fed the chow diet until the fasting period. Eight *Plin4*^{+/+} mice and seven *Plin4*^{-/-} mice were fasted by food deprivation for 24 hours at ~15 weeks of age. Gene expression of Plin family members in liver was analysed with RT-qPCR, related to the expression of TBP. Data are shown as Means \pm SEM (n = 8 mice in each group, except for the *Plin4*^{-/-} fasting group; n = 7 mice). Statistical significance was determined by Bonferroni's multiple comparison test (*p < 0,05; **p < 0,01; ***p < 0,001). RT-qPCR: Quantitative reverse transcription polymerase chain reaction; TBP: TATA binding protein; SEM: standard error of the mean.

Genes involved in lipid metabolism

In response to fasting, hepatic lipogenesis is known to be repressed, this due to high uptake of NEFAs delivered from the circulation in response to active lipolysis in adipose tissue. As expected, the mRNA levels of *Srebp1a*, *Srebp1c*, *Chrebp* and *Fasn* observed in fasting mice were reduced due to the energetic shift from fed to fasted, and the lack of glucose and fatty acids as substrates for lipogenesis (figure 9 E, F, G and H). The mRNA levels of *Dgat2*, *Ldlr*, *Abca1* and *Abcg1* were also lower in fasted mice compared to fed (figure 9 J, L, M and N). This gene expression pattern indicates reduced lipogenesis and reduced hepatic uptake of cholesterol (downregulation in *Ldlr*, *Abca1* and *Abcg1*) in fasted mice compare to fed mice.

Hepatic uptake of NEFAs in response to fasting will provide sufficient ligand availability for *Ppara*, which is a fatty acid sensing transcription factor highly expressed in liver (90, 91). As expected, the gene expression of *Ppara* were increased during fasting in *Plin4*^{+/+} mice, but the same increase was not observed in *Plin4*^{-/-} mice (figure 9 A). This may indicate lower hepatic uptake of NEFAs from the circulation in fasted mice where *Plin4* is absent, and subsequently lower activation of *Ppara*.

Chow diet is composed of 58 E% carbohydrates, 18 E% fat and 24 E% protein, similar composition to the Western control diet (see table 5). The mRNA expression of *Fasn* was significantly downregulated in *Plin4*^{-/-} mice receiving chow diet compared to *Plin4*^{+/+} mice (figure 9 H). Same tendency was seen for *Srebp1c* (figure 9 F), although non-significant. Similar results were found in *Plin4*^{-/-} mice receiving Western control diet, shown in figure 4. These results may indicate the role of *Plin4* in lipogenesis when fat is low and carbohydrates are in excess.

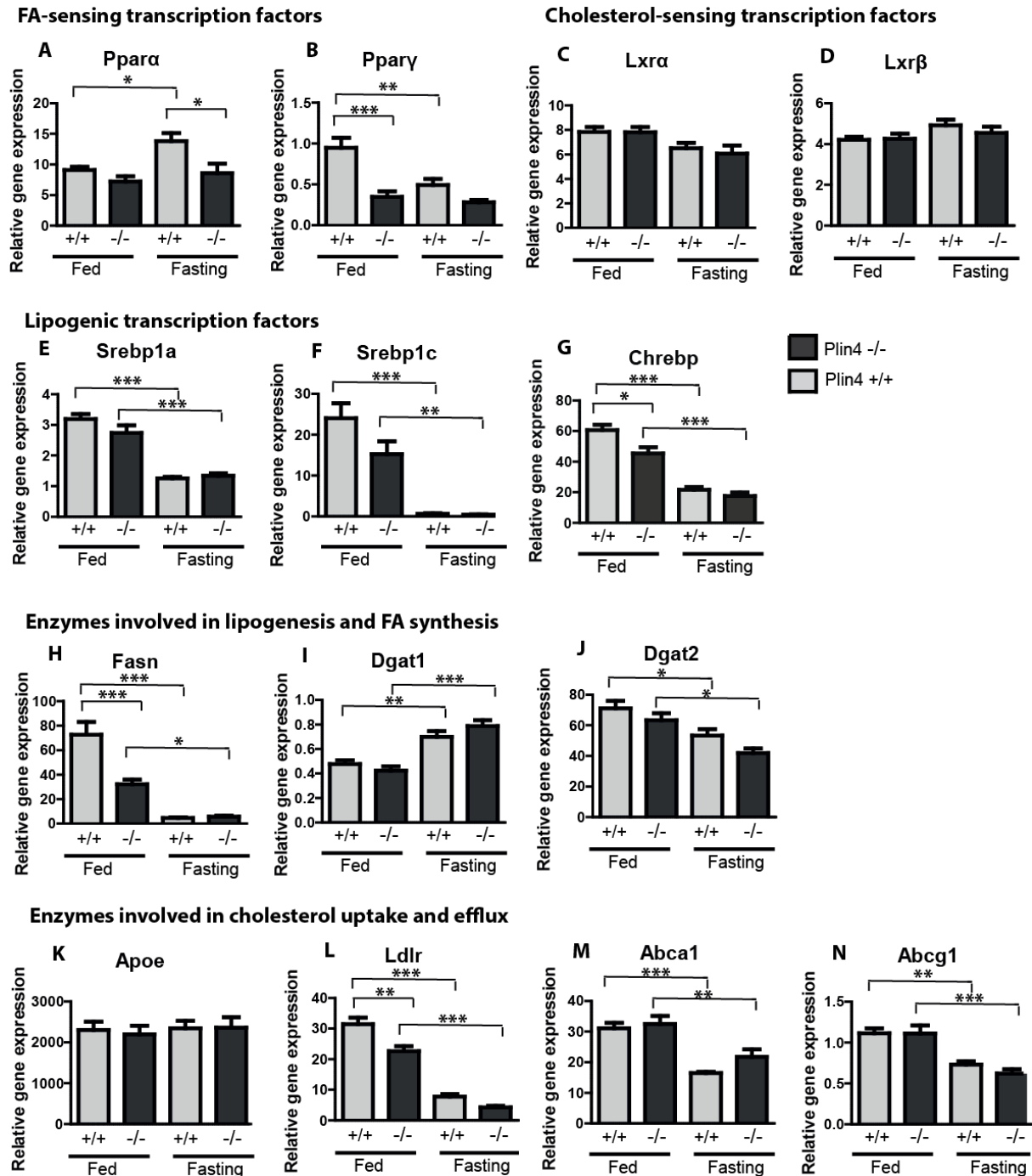


Figure 9. Hepatic expression of genes involved in lipid metabolism, fasting intervention. The intervention included 16 *Plin4*^{+/+} and 15 *Plin4*^{-/-} male mice. All mice were fed the chow diet until the fasting period. Eight *Plin4*^{+/+} mice and seven *Plin4*^{-/-} mice were fasted by food deprivation for 24 hours at ~15 weeks of age. Expression of genes involved in lipid metabolism were analysed with RT-qPCR, related to the expression of TBP. Data are shown as Means ± SEM (n = 8 mice in each group, except for the *Plin4*^{-/-}-fasting group; n = 7 mice). Statistical significance was determined by Bonferroni's multiple comparison test (*p < 0,05; **p < 0,01; ***p < 0,001). RT-qPCR: Quantitative reverse transcription polymerase chain reaction; TBP: TATA binding protein; SEM: standard error of the mean.

3.3.3 Content of triacylglycerol and total cholesterol

We also wanted to investigate how absent of *Plin4* affect prolonged fasting in terms of accumulation of lipids in liver. It is known that fasting conditions increase the accumulation of TAG in the liver due to active lipolysis in adipose tissue and subsequently hepatic uptake (89).

No significant difference between the genotypes were seen in content of TAG or total cholesterol in mice receiving chow diet (figure 10 A and B). The switch between fed and fasted state resulted in an increase in content of TAG in both *Plin4*^{+/+} and *Plin4*^{-/-} mice, but the accumulation of TAG was significantly lower in *Plin4*^{-/-} mice compared to *Plin4*^{+/+} mice (figure 10 A). Potential explanations for reduced hepatic TAG content are increased β -oxidation, increased secretion of VLDL particles, and reduced uptake of NEFAs.

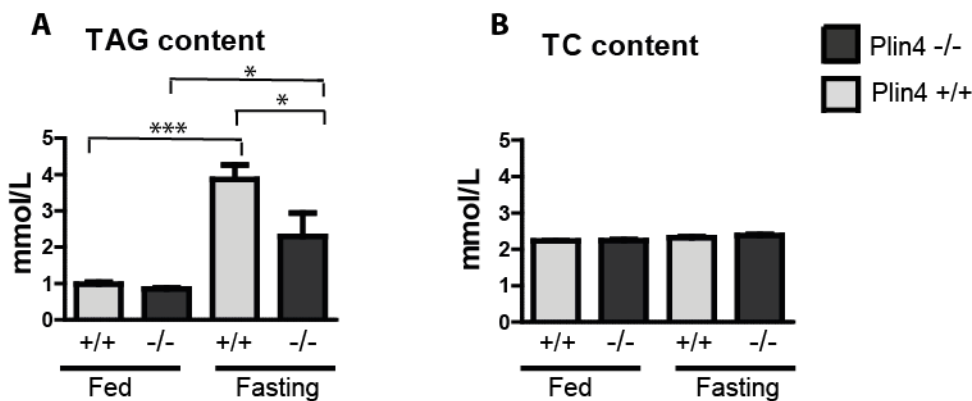


Figure 10. Hepatic content of triacylglycerol and total cholesterol, fasting intervention. The intervention included 16 *Plin4*^{+/+} and 15 *Plin4*^{-/-} male mice. All mice were fed the chow diet until the fasting period. Eight *Plin4*^{+/+} mice and seven *Plin4*^{-/-} mice were fasted by food deprivation for 24 hours at ~15 weeks of age. Data are shown as Means \pm SEM (n = 8 mice in each group, except for the *Plin4*^{-/-} fasting group; n = 7 mice). Statistical significance was determined by Bonferroni's multiple comparison test (*p < 0,05; **p < 0,01; ***p < 0,001). TAG: triacylglycerol; TC: total cholesterol; SEM: standard error of the mean.

4 Discussion

This master thesis has investigated the role of *Plin4* in adipose tissue and liver by comparing *Plin4*^{+/+} and *Plin4*^{-/-} mice receiving various diets or food withdraw (fasting). Molecular analyses have focused on gene expression, LD morphology, and content of TAG and total cholesterol in liver and adipose tissue.

The main finding presented in this master thesis is the lower expression of genes involved in hepatic lipogenesis seen in the absence of *Plin4*. This reduction was seen in *Plin4*^{-/-} female mice receiving Western control diet and *Plin4*^{-/-} male mice receiving chow diet. Secondly, lower expression of *Plin5* in liver were seen in *Plin4*^{-/-} male mice receiving high-fat diet, *Plin4*^{-/-} female mice receiving Western control diet and fasted *Plin4*^{-/-} male mice. Additionally, hepatic gene expression of *Ppara* was not induced in fasted *Plin4*^{-/-} male mice compared to fasted *Plin4*^{+/+} mice. There were also seen lower hepatic content of TAG in fasted *Plin4*^{-/-} male mice, which may be related to the changes seen in gene expression. Lastly, mice lacking *Plin4* had a higher body weight loss and less remaining epididymal fat mass after fasting compared to *Plin4*^{+/+} mice.

4.1 Discussion of the methodology

4.1.1 Animal knock-out models

In this master thesis *Plin4*^{-/-} mice were compared to *Plin4*^{+/+} mice to study potential functions of *Plin4*. *Plin4*^{-/-} mice were generated using the standard gene disrupting procedure in 129/Sv ES cells. *Plin4*^{-/-} mice have been backcrossed to a congenic strain (the C57BL/6J strain) for more than 10 generations. In all experiments, *Plin4*^{+/+} mice from the same breeding colony were used as controls. The mice should therefore be genetically similar, except for the lack of a functional *Plin4* gene. Validation of each animal used in these studies was performed by RT-qPCR analysis of *Plin4* gene expression. There were no detectable mRNA levels of *Plin4* in either of the mice included, except for one mouse that was excluded from the study based on these qPCR results. Knock-out mice models are very often used to investigate gene function. Due to the greatly overlapping genomes, data from mouse models will often give us valuable insight in protein functions in humans.

4.1.2 Quantitative reverse transcription polymerase chain reaction

The RT-qPCR method has been used to compare gene expression of various RNAs between mice receiving different diets. The advantages of the RT-qPCR is its high sensitivity and reproducibility, as well as its cost effectiveness and simple performance (92). The RT-qPCR is although sensitive to pipetting error, which may be a limitation in this thesis due to unexperienced master student as data collector.

To obtain high-quality RNA, the RNA isolation step requires accurate transfer of RNA supernatant to avoid contamination with DNA. The RNA isolation method used in this master thesis involves a DNase-reaction step. This enzyme catalyses the hydrolytic cleavage of bindings in the DNA molecule, and DNA that still remains in the samples will be degraded. This lowers the risk for DNA contamination.

The extraction step to remove proteins prior to application to the NucleoSpin RNA column contains phenols and some of the buffers contain guanidine. If the removal of phenols is incomplete, cDNA synthesis might be inhibited and therefore affected in a negative manner. The quality of cDNA is dependent on good quality RNA, and the risk of RNA degradation increases if phenol is present. Each RNA sample was analysed with the Nano Drop ND-1000 spectrophotometer (Thermo Scientific, Waltham, MA) to quantify RNA content and analyse pureness. This lowers the risk for undiscovered contamination, which would have limited the power of the RT-qPCR data. To assess RNA quality, 260/280 and 260/230 ratios were analysed and an average of the two ratios below 2,0 was considered insufficient, and the RNA isolation was repeated.

Two controls were made in the set-up for cDNA synthesis. One control contained template made by 1/3 of three randomly chosen samples and no reverse transcriptase enzyme (no-RT). This control was made to check for DNA contamination in isolated RNA samples. The second control was made without template (RNA sample) to control for contamination of solutions used in the reaction mixture. These controls were analysed for each gene expression assay, which makes it possible to identify primer design errors, methodological mistakes in the cDNA synthesis, or contamination problems.

Relative quantification of qPCR data requires a normalization of gene expression levels against expression of a reference gene to obtain reliable results. The reference gene should be

ubiquitously expressed, and a so-called housekeeping gene is often chosen. A housekeeping gene is expressed in almost all tissues and is not transcriptionally regulated under the experimental conditions being tested (93). The most suited reference gene depends on which tissue that is investigated and the specie of interest. In this study, TBP was chosen as reference gene based on the similar expression levels between the groups of mice, as well as the researcher groups previous experience with this gene in these two tissues. This is a general transcription factor with specific binding to a DNA sequence called TATA-box (94). The use of TBP as reference gene has shown to be suited in mice liver and WAT (95, 96) and was shown to be one of the three most stable gene in all mouse tissues investigated in Sun *et. al.* (96). It may although not be the most suited reference gene in all tissues and with all diets. GeNorm analysis can be used to evaluate potential reference genes for *normalization* purposes (97). Such an analysis was not performed in this study, which may be a limitation to the accuracy of the gene expression data, alternatively, two reference genes may be used simultaneously (86, 94). This study has only used one reference gene for gene expression analyses, which may be another limitation.

The main results in this master thesis are based on RT-qPCR data. RT-qPCR is a well-proven method to investigate changes in mRNA levels between different groups of mice, but the fold change may not correspond to protein levels due to binding of coactivators, corepressors and posttranslational regulation. The lack of protein expression levels is a limitation to this study.

4.1.1 Measuring hepatic content of triacylglycerol and total cholesterol

Quantitative hepatic lipid analysis was performed using colorimetric detection kits to measure content of TAG (Triglycerides Enzymatique PAP150, Biomerieux) and total cholesterol (Cholesterol 1600, ERBA Diagnostics, MaxMat) in homogenate of liver tissue. Before measuring content of lipids, the homogenates were frozen at -80°C. After thawing, all samples were sonicated to fully dissolve the homogenised samples. Based on the experienced insufficient dissolving with mechanical homogenisation, sonication may be preferred as an additional step after homogenisation with beads, prior to analyses of lipid content in whole tissue samples.

The two kits used in this master thesis does not require a standard curve for quantification of lipids, but contain an equation for calculation based on a blank sample and one standard. A

standard curve was made in one of the experiments to validate the use of the equation given in the manufacture protocols. The results were similar. To save reagents, the equations from the standard protocols were used without making a standard curve for the rest of the experiment.

4.1.2 Histology

To examine hepatic lipid content by histology, liver tissue fixed with 4% PFA was cut in thin sections stained and mounted to microscopic slides. Sucrose solutions (10, 20 and 30 % sucrose) were used to substitute water within the tissue pieces to prevent tissue destruction when freezing. This is a commonly used procedure for cryoprotection to avoid the formation of ice crystals that will destroy cell structure and in our case, the LD structure.

OCT was used as embedding medium. This is the embedding medium designed for cryosections. Cryosectioning was performed rather than other sectioning methods, because the histological objective was to investigate LD morphology. Paraffin and resin are two commonly used alternative tissue embedding media (98). These embedding procedures use harsh organic solvents for tissue treatment, which would remove all neutral lipids from the LD core and leave an empty “shell”. This would potentially destroy the LD structure and make it impossible to stain lipids. These alternative methods were therefore not convenient in this case.

Bodipy (493/503), Phalloidin-CF568 conjugate and Hoechst were used as dyes. Bodipy has been used previously to stain LDs (62, 63, 87), Phalloidin may be used to stain cell membranes, (99) while Hoechst is often used to stains double stranded DNA and visualise the nuclei (100). The use of all three dyes at once has been previously tested in the research group and was found to provide adequate results in studying LD morphology. Staining separately has not provided obvious improvement on image quality.

The microscopic slides were scanned under a 20 x objective with an Axio Scan Z1 system (Zeiss). The digital images were analysed in Zen 2.3 imaging software (blue edition). The images were chosen manually, which limits the objectiveness in the results. The images were although required for representative purpose only, not for quantification. The histological objective was to compare LD morphology with measured lipid content, and manually chosen representative images are sufficient for that purpose.

4.1.3 Statistical methods and sample size

The one-way ANOVA with Bonferroni's Multiple Comparison test as post-hoc test were used to evaluate statistical significance between more than three independent groups. One-way ANOVA is a parametric test with assumptions of normality, equal variance and independent samples (101). Parametric tests are preferred if possible, rather than non-parametric tests such as Mann-Whitney test and Kruskal-Wallis, due to higher statistical power and the ability to test group means rather than group medians. Similar studies to this master thesis do report their results as Means \pm SEM. To be able to compare our data to previous studies, testing of group means by parametric testing was preferred.

It is not possible to properly test if the data were normally distributed with only eight mice per group. Numerically testing of normality was therefore not relied on. In cases where there were doubt if specific results were normally distributed, we assumed that they would be if the number of animals were increased to meet the sample size guidelines for the use of one-way ANOVA (with potential non-normal distributed data) (101). This may be a limitation to the statistical evaluation of the qPCR results.

The sample size (number of animals) was based on the research group's prior experience with similar animal experiments. Backcrossing of the model has generated genetically highly similar individuals with the main difference being the presence or absence of the *Plin4* gene. This lower individual variation and reduced the number of individuals required, compared to studying individuals representing a population. To fulfil ethical requirement for animal experiments, the number of animals used should be as low as possible. The number of animals per group used in this master thesis (7-8) is sufficient to demonstrate biological relevant differences, and was also the number of mice available when data collection was performed.

4.2 Discussion of the results

4.2.1 Main results

Alterations in expression of genes involved in lipogenesis

Our study reports alterations in expression of genes involved in hepatic lipogenesis when *Plin4* is absent. Gene expression of *Srebp1a*, *Srebp1c*, *Fasn*, *Dgat1* and *Dgat2* were downregulated in female *Plin4*^{-/-} receiving Western control diet, compared to *Plin4*^{+/+} mice. These transcription factors and target genes are involved in the lipogenesis and synthesis of fatty acids (49). In dietary states where the dietary content of fat is low and carbohydrates are high (as with the Western control diet), increased gene expression of these enzymes is expected to occur to active hepatic lipogenesis. This was not seen in *Plin4*^{-/-} mice, which indicates that the lipogenic response to low fat and high carbohydrate is altered in the absence of *Plin4*. A similar gene expression pattern was seen in male *Plin4*^{-/-} mice receiving chow diet (similar diet composition to the Western control diet) in the fasting intervention. The consistent observations in two experiments indicate a potential role of *Plin4* for regulation of hepatic lipogenesis when fat is low and carbohydrates are in excess. This is a novel observation, not previously reported in existing literature investigating *Plin4* function.

Some previous studies have shown that absence of Plin family members affect mRNA levels of genes involved in lipid metabolism, but changes in gene expression patterns are scarcely investigated. Schweiger *et. al.* show that overexpression of *Plin5* reduces gene expression of genes involved in fatty acid oxidation (78). Chen *et. al.* investigated expression of genes involved in uptake of glucose and fatty acids to the heart, as well as genes involved in β -oxidation (76). No change in gene expression was reported by Chen *et. al.*

Downregulated gene expression of *Plin5*

Our study reports a lack of induction in hepatic gene expression of *Plin5* in mice receiving high-fat diet, Western control diet, and fasted mice, when *Plin4* was absent. Our findings replicate findings of another study. Chen *et. al.* reports that the gene expression of *Plin5* is reduced in the heart, white adipose tissue and liver in *Plin4*^{-/-} mice compared to *Plin4*^{+/+} mice (76). Chen *et. al.* also report reduction of *Plin5* at protein levels, which our study has not investigated. One hypothesis suggested by Chen *et. al.* was that the gene disrupting method

for the removal of functional *Plin4* resulted in reduced gene expression of *Plin5* as well (76). If this was the case, the opposite scenario seems reasonable, with downregulation of *Plin4* when *Plin5* is absent. Kuramoto *et. al.* show no downregulation of *Plin4* when *Plin5* is absent (80). The underlying explanation why the expression of *Plin5* is downregulated when *Plin4* is absent is still unknown.

Our findings for *Plin4* in liver differ from other studies where the absence of one of the other Plin family members rather results in a compensatory increased expression of other members (70, 102). Sztalryd *et. al.* show that the absence of *Plin1* increases the gene expression of *Plin2* in adipocytes (70). Wang *et. al.* show that the expression of *Plin3* is upregulated when *Plin2* is downregulated (102). Our study did although observe an increase in *Plin5* expression in epididymal fat in *Plin4*^{-/-} male mice receiving high-fat diet (figure 1 E), but this increase was not investigated further.

Altered response to fasting

Our study identified altered response to fasting when *Plin4* is absent. In the absence of *Plin4*, hepatic gene expression of *Ppara* were lower in *Plin4*^{-/-} male mice fasted for 24 hours, compared to fasted *Plin4*^{+/+} mice. Gene expression of *Ppara* and *Ppara* target genes usually increase in response to fasting due to high levels of NEFAs (91) delivered to the liver from active lipolysis in adipose tissue. High uptake of NEFAs to liver will normally provide increased ligand availability for *Ppara* and sequentially increased expression of *Ppara*, but this seems not to occur in mice lacking *Plin4*. This indicates a lower hepatic uptake of NEFAs from the circulation in fasted mice where *Plin4* is absent, or alterations in signals that would normally activate expression of *Ppara*. *Ppara*s are known to regulate gene expression of *Plin1*, *Plin2* and *Plin5* (64, 65, 91). We also observed significantly lower mRNA levels of *Plin5* in fasted *Plin4*^{-/-} male mice compared to *Plin4*^{+/+} mice, and the same tendency was seen for *Plin1* and *Plin2*. The lower gene expression of Plin family members therefore corresponds to lower gene expression of *Ppara*.

In agreement with potential reduced levels of NEFAs in the absence of *Plin4*, the accumulation of TAG was found to be significantly lower in *Plin4*^{-/-} mice compared to *Plin4*^{+/+} mice. Potential explanations for lower TAG content are increased β -oxidation, increased secretion of VLDL particles, or reduced hepatic uptake of NEFAs. Due to a lack of induction of *Ppara* expression, reduced hepatic uptake of NEFAs from the circulation seems

likely, resulting in altered hepatic fasting response when *Plin4* is absent. A part of this effect may be caused by insufficient fat depots. If prolonged fasting metabolise the majority of TAG stored in adipocyte LDs, the supply of NEFAs to the liver will be reduced. When we investigated data from individual mice in the fasting intervention, we observed that mice with the lowest WAT depots remaining after fasting had the lowest hepatic TAG levels (results not shown). Based on this, we conclude that insufficient WAT depots may be linked to the lower levels of TAG in fasted *Plin4*^{-/-} mice compared to *Plin4*^{+/+} mice, rather than the absence of *Plin4*.

Two previous studies have reported reduced accumulation of TAG when Plin family members are absent. Chang *et. al.* reports that the absence of *Plin2* lowers TAG content in liver by 25-60 % (71) due to increased secretion of VLDL particles. Chen *et. al.* reports significantly reduced cardiac content of TAG in *Plin4*^{-/-} mice (76) and same tendency was reported in liver. The reduced cardiac lipid content reported by Chen *et. al.* may although be caused by the simultaneously reduced gene expression of *Plin5*, since lack of *Plin5* results in lower levels of cardiac TAG (80).

Differences in epididymal fat mass

In the fasting intervention study, where mice received chow diet, we observed less epididymal fat mass in male *Plin4*^{-/-} mice compared to *Plin4*^{+/+} mice. This indicates that mice lacking *Plin4* may have reduced ability to store TAG in epididymal fat reservoirs when eating certain diets. No change in subcutaneous fat mass was observed, but whole body fat mass should be investigated further before making any conclusions. Another *Plin4* null study did not observe any differences in fat composition (76) and reported similar body weight, total fat mass and amount of WAT in *Plin4*^{+/+} and *Plin4*^{-/-} mice. The difference in amount of epididymal fat observed in the present study may be an interesting phenotype of mice lacking *Plin4*, but as the same difference were not seen in all experiments, no conclusions were made.

4.2.2 Clinical relevance

Increased accumulation of neutral lipids in LDs found in visceral and ectopic fat depots, such as liver and muscle, are strongly related to obesity and associated metabolic diseases. Plins are involved in the lipid storing ability of the LDs by regulating lipolysis (58). Plins may therefore play an important role in the development of diseases related to abnormal lipid

metabolism. There are previously found that manipulation of the expression of these Plin family members may affect these metabolic diseases. Absence of *Plin1* results in mice resistant to diet-induced obesity (69), absence of *Plin2* protects against diet-induced fatty liver disease (72), absence of *Plin3* changes LD morphology (74) and the absence of *Plin5* has shown to reduces lipid content in the heart (78, 80, 81). These studies supports the importance of further investigating the role of the Plin family members as potential therapeutic targets in treatment of obesity and obesity related diseases.

5 Conclusion

Our study observed lower expression of genes involved in hepatic lipogenesis when *Plin4* was absent. This reduced expression was seen in *Plin4*^{-/-} mice receiving the Western control diet and the chow diet given in the fasting intervention. Both of these diets are low in fat and high in carbohydrate. Gene expression analyses in the high-fat diet intervention should be examined in future studies to determine if genes involved in hepatic lipogenesis is lower expressed in *Plin4*^{-/-} mice in the low-fat control diet group, similar to what we find with the two other carbohydrate-rich and low-fat diets in this study. The low-fat control diet consists of even less fat than the chow diet and Western control diet (10 E% versus 18 and 20 E% respectively), and it would be interesting to know if the expression of genes involved in hepatic lipogenesis are even lower expressed in mice receiving the low-fat control diet when *Plin4* is absent. Future studies should also include Western blot analyses to confirm that changes seen in at the transcriptional level corresponds to similar changes post-transcriptionally.

Our study reports lower expression of *Plin5* when *Plin4* is absent. The underlying explanation for why the expression of *Plin5* is reduced in *Plin4*^{-/-} mice compared to *Plin4*^{+/+} mice is still unknown. This could be a focus for future studies, where variation in diets is linked to differences in *Plin5* gene expression in different tissues. Future studies should also include Western blot analyses to confirm that changes seen in at the transcriptional level corresponds to similar changes post-transcriptionally.

Our study identified altered response to fasting when *Plin4* was absent. Hepatic gene expression of *Ppara* were lower in *Plin4*^{-/-} male mice fasted for 24 hours, compared to fasted *Plin4*^{+/+} mice. The most likely explanations are lower hepatic uptake of NEFAs from the circulation in fasted mice when *Plin4* is absent, or alterations in signals that would normally activate expression of *Ppara*. In agreement with potential reduced levels of NEFAs in the absence of *Plin4*, the accumulation of TAG in liver was significantly lower in fasted *Plin4*^{-/-} male mice compared to *Plin4*^{+/+} mice. Due to the differences in epididymal fat depots in this study, we cannot conclude based on this experiment alone, since insufficient WAT depots potentially affects expression of *Pparα* and substrate availability for hepatic TAG synthesis. The experiment should be repeated with mice starting with a higher epididymal fat depot and should also include Western blot analyses to confirm that changes seen in at the

transcriptional level corresponds to similar changes post-transcriptionally. Hepatic levels of NEFAs and glycerol should also be measured in future studies to investigate potential explanations in altered hepatic TAG content. Based on the results reported in the present study, the combination of low fat and high carbohydrate or lack of energy (fasting) should be in focus.

Our study observed differences in the amount of epididymal fat between *Plin4*^{+/+} and *Plin4*^{-/-} mice. This may be an interesting phenotype of mice lacking *Plin4*, but this altered fat composition was only observed in one of the three studies investigated in this master thesis. No conclusions should therefore be made based on these results, and the fasting study should be repeated to be able to conclude regarding a potential role of *Plin4* in fat mass composition. Future studies should measure whole body fat masses to investigate potential alteration when *Plin4* is absent.

Based on the results reported in our study, it seems likely that *Plin4* is important for expression of genes involved in hepatic lipogenesis in dietary conditions where fat is low and carbohydrates are high. *Plin4* may also be important in liver in the response to fasting. Further investigations are needed to fully understand the role of *Plin4* in lipid metabolism.

References

1. Krahmer N, Farese RV, Jr., Walther TC. Balancing the fat: lipid droplets and human disease. *EMBO molecular medicine*. 2013;5(7):973-83.
2. Lee YH, Mottillo EP, Granneman JG. Adipose tissue plasticity from WAT to BAT and in between. *Biochimica et biophysica acta*. 2014;1842(3):358-69.
3. Oelkrug R, Polymeropoulos ET, Jastroch M. Brown adipose tissue: physiological function and evolutionary significance. *Journal of comparative physiology B, Biochemical, systemic, and environmental physiology*. 2015;185(6):587-606.
4. Chondronikola M, Sidossis LS. Brown and beige fat: From molecules to physiology. *Biochimica et biophysica acta Molecular and cell biology of lipids*. 2018.
5. Rosen ED, Spiegelman BM. Adipocytes as regulators of energy balance and glucose homeostasis. *Nature*. 2006;444(7121):847-53.
6. Ahima RS. Adipose tissue as an endocrine organ. *Obesity (Silver Spring, Md)*. 2006;14 Suppl 5:242s-9s.
7. Konige M, Wang H, Sztalryd C. Role of adipose specific lipid droplet proteins in maintaining whole body energy homeostasis. *Biochimica et biophysica acta*. 2014;1842(3):393-401.
8. Sztalryd C, Kimmel AR. Perilipins: lipid droplet coat proteins adapted for tissue-specific energy storage and utilization, and lipid cytoprotection. *Biochimie*. 2014;96:96-101.
9. Grousse A, Langin D. Adipocyte lipases and lipid droplet-associated proteins: insight from transgenic mouse models. *International journal of obesity (2005)*. 2012;36(4):581-94.
10. Bellanti F, Villani R, Facciorusso A, Vendemiale G, Serviddio G. Lipid oxidation products in the pathogenesis of non-alcoholic steatohepatitis. *Free radical biology & medicine*. 2017;111:173-85.
11. Bjorndal B, Burri L, Staalesen V, Skorve J, Berge RK. Different adipose depots: their role in the development of metabolic syndrome and mitochondrial response to hypolipidemic agents. *Journal of obesity*. 2011;2011:490650.
12. Greenberg AS, Coleman RA, Kraemer FB, McManaman JL, Obin MS, Puri V, et al. The role of lipid droplets in metabolic disease in rodents and humans. *The Journal of clinical investigation*. 2011;121(6):2102-10.
13. Conte M, Franceschi C, Sandri M, Salvioli S. Perilipin 2 and Age-Related Metabolic Diseases: A New Perspective. *Trends in endocrinology and metabolism: TEM*. 2016;27(12):893-903.
14. World Health Organization. Obesity and overweight 2018 [updated 16.02.18;06.11.18]. Available from: <https://www.who.int/news-room/fact-sheets/detail/obesity-and-overweight>.
15. Heindel JJ, Blumberg B, Cave M, Machtinger R, Mantovani A, Mendez MA, et al. Metabolism disrupting chemicals and metabolic disorders. *Reproductive toxicology (Elmsford, NY)*. 2017;68:3-33.
16. Sam S, Mazzone T. Adipose tissue changes in obesity and the impact on metabolic function. *Translational research : the journal of laboratory and clinical medicine*. 2014;164(4):284-92.

17. World Health Organization W. Obesity: preventing and managing the global epidemic. Report of a WHO consultation. World Health Organization technical report series. 2000;894:i-xii, 1-253.
18. Juza RM, Pauli EM. Clinical and surgical anatomy of the liver: a review for clinicians. Clinical anatomy (New York, NY). 2014;27(5):764-9.
19. Mahan LKR, J.L.; . Krause's Food & The Nutrition Care Process, 14th edition In: Inc E, editor. Krause's Food & The Nutrition Care Process, 14th edition Fourteenth edition ed. St. Louis, Missouri Elsevier Inc; 2017.
20. Leavens KF, Birnbaum MJ. Insulin signaling to hepatic lipid metabolism in health and disease. Critical reviews in biochemistry and molecular biology. 2011;46(3):200-15.
21. Jones JG. Hepatic glucose and lipid metabolism. Diabetologia. 2016;59(6):1098-103.
22. Finn PF, Dice JF. Proteolytic and lipolytic responses to starvation. Nutrition (Burbank, Los Angeles County, Calif). 2006;22(7-8):830-44.
23. Wang C, Zhao Y, Gao X, Li L, Yuan Y, Liu F, et al. Perilipin 5 improves hepatic lipotoxicity by inhibiting lipolysis. Hepatology (Baltimore, Md). 2015;61(3):870-82.
24. Loomba R, Sanyal AJ. The global NAFLD epidemic. Nature reviews Gastroenterology & hepatology. 2013;10(11):686-90.
25. Ipsen DH, Lykkesfeldt J, Tveden-Nyborg P. Molecular mechanisms of hepatic lipid accumulation in non-alcoholic fatty liver disease. Cellular and molecular life sciences : CMLS. 2018;75(18):3313-27.
26. Kersten S. Mechanisms of nutritional and hormonal regulation of lipogenesis. EMBO reports. 2001;2(4):282-6.
27. Zechner R, Zimmermann R, Eichmann TO, Kohlwein SD, Haemmerle G, Lass A, et al. FAT SIGNALS--lipases and lipolysis in lipid metabolism and signaling. Cell metabolism. 2012;15(3):279-91.
28. Bolsoni-Lopes A, Alonso-Vale MI. Lipolysis and lipases in white adipose tissue - An update. Archives of endocrinology and metabolism. 2015;59(4):335-42.
29. Coleman RA, Lee DP. Enzymes of triacylglycerol synthesis and their regulation. Progress in lipid research. 2004;43(2):134-76.
30. Lass A, Zimmermann R, Oberer M, Zechner R. Lipolysis - a highly regulated multi-enzyme complex mediates the catabolism of cellular fat stores. Progress in lipid research. 2011;50(1):14-27.
31. Lass A, Zimmermann R, Haemmerle G, Riederer M, Schoiswohl G, Schweiger M, et al. Adipose triglyceride lipase-mediated lipolysis of cellular fat stores is activated by CGI-58 and defective in Chanarin-Dorfman Syndrome. Cell metabolism. 2006;3(5):309-19.
32. Chakrabarti P, Kim JY, Singh M, Shin YK, Kim J, Kumbrink J, et al. Insulin inhibits lipolysis in adipocytes via the evolutionarily conserved mTORC1-Egr1-ATGL-mediated pathway. Molecular and cellular biology. 2013;33(18):3659-66.
33. Yamaguchi T, Omatsu N, Matsushita S, Osumi T. CGI-58 interacts with perilipin and is localized to lipid droplets. Possible involvement of CGI-58 mislocalization in Chanarin-Dorfman syndrome. The Journal of biological chemistry. 2004;279(29):30490-7.
34. Subramanian V, Rothenberg A, Gomez C, Cohen AW, Garcia A, Bhattacharyya S, et al. Perilipin A mediates the reversible binding of CGI-58 to lipid droplets in 3T3-L1 adipocytes. The Journal of biological chemistry. 2004;279(40):42062-71.
35. Brown AL, Mark Brown J. Critical roles for alpha/beta hydrolase domain 5 (ABHD5)/comparative gene identification-58 (CGI-58) at the lipid droplet interface and beyond. Biochimica et biophysica acta Molecular and cell biology of lipids. 2017;1862(10 Pt B):1233-41.

36. Granneman JG, Moore HP, Granneman RL, Greenberg AS, Obin MS, Zhu Z. Analysis of lipolytic protein trafficking and interactions in adipocytes. *The Journal of biological chemistry*. 2007;282(8):5726-35.
37. Sahu-Osen A, Montero-Moran G, Schittmayer M, Fritz K, Dinh A, Chang YF, et al. CGI-58/ABHD5 is phosphorylated on Ser239 by protein kinase A: control of subcellular localization. *Journal of lipid research*. 2015;56(1):109-21.
38. Greenberg AS, Egan JJ, Wek SA, Garty NB, Blanchette-Mackie EJ, Londos C. Perilipin, a major hormonally regulated adipocyte-specific phosphoprotein associated with the periphery of lipid storage droplets. *The Journal of biological chemistry*. 1991;266(17):11341-6.
39. Miyoshi H, Souza SC, Zhang HH, Strissel KJ, Christoffolete MA, Kovsan J, et al. Perilipin promotes hormone-sensitive lipase-mediated adipocyte lipolysis via phosphorylation-dependent and -independent mechanisms. *The Journal of biological chemistry*. 2006;281(23):15837-44.
40. Yamaguchi T, Omatsu N, Morimoto E, Nakashima H, Ueno K, Tanaka T, et al. CGI-58 facilitates lipolysis on lipid droplets but is not involved in the vesiculation of lipid droplets caused by hormonal stimulation. *Journal of lipid research*. 2007;48(5):1078-89.
41. Granneman JG, Moore HP, Krishnamoorthy R, Rathod M. Perilipin controls lipolysis by regulating the interactions of AB-hydrolase containing 5 (Abhd5) and adipose triglyceride lipase (Atgl). *The Journal of biological chemistry*. 2009;284(50):34538-44.
42. Han L, Shen WJ, Bittner S, Kraemer FB, Azhar S. PPARs: regulators of metabolism and as therapeutic targets in cardiovascular disease. Part II: PPAR-beta/delta and PPAR-gamma. *Future cardiology*. 2017;13(3):279-96.
43. Pawlak M, Lefebvre P, Staels B. Molecular mechanism of PPARalpha action and its impact on lipid metabolism, inflammation and fibrosis in non-alcoholic fatty liver disease. *Journal of hepatology*. 2015;62(3):720-33.
44. Janani C, Ranjitha Kumari BD. PPAR gamma gene--a review. *Diabetes & metabolic syndrome*. 2015;9(1):46-50.
45. Zelcer N, Tontonoz P. Liver X receptors as integrators of metabolic and inflammatory signaling. *The Journal of clinical investigation*. 2006;116(3):607-14.
46. Steffensen KR, Gustafsson JA. Putative metabolic effects of the liver X receptor (LXR). *Diabetes*. 2004;53 Suppl 1:S36-42.
47. Zhang L, Rajbhandari P, Priest C, Sandhu J, Wu X, Temel R, et al. Inhibition of cholesterol biosynthesis through RNF145-dependent ubiquitination of SCAP. *eLife*. 2017;6.
48. Jeong YS, Kim D, Lee YS, Kim HJ, Han JY, Im SS, et al. Integrated expression profiling and genome-wide analysis of ChREBP targets reveals the dual role for ChREBP in glucose-regulated gene expression. *PloS one*. 2011;6(7):e22544.
49. Eberle D, Hegarty B, Bossard P, Ferre P, Foulle F. SREBP transcription factors: master regulators of lipid homeostasis. *Biochimie*. 2004;86(11):839-48.
50. Horton JD, Goldstein JL, Brown MS. SREBPs: activators of the complete program of cholesterol and fatty acid synthesis in the liver. *The Journal of clinical investigation*. 2002;109(9):1125-31.
51. Brasaemle DL. Thematic review series: adipocyte biology. The perilipin family of structural lipid droplet proteins: stabilization of lipid droplets and control of lipolysis. *Journal of lipid research*. 2007;48(12):2547-59.
52. Walther TC, Farese RV, Jr. Lipid droplets and cellular lipid metabolism. *Annual review of biochemistry*. 2012;81:687-714.
53. Schulze RJ, Sathyanarayan A, Mashek DG. Breaking fat: The regulation and mechanisms of lipophagy. *Biochimica et biophysica acta Molecular and cell biology of lipids*. 2017;1862(10 Pt B):1178-87.

54. Kimmel AR, Sztalryd C. The Perilipins: Major Cytosolic Lipid Droplet-Associated Proteins and Their Roles in Cellular Lipid Storage, Mobilization, and Systemic Homeostasis. *Annual review of nutrition*. 2016;36:471-509.
55. Sztalryd C, Brasaemle DL. The perilipin family of lipid droplet proteins: Gatekeepers of intracellular lipolysis. *Biochimica et biophysica acta Molecular and cell biology of lipids*. 2017;1862(10 Pt B):1221-32.
56. Ohsaki Y, Cheng J, Suzuki M, Shinohara Y, Fujita A, Fujimoto T. Biogenesis of cytoplasmic lipid droplets: from the lipid ester globule in the membrane to the visible structure. *Biochimica et biophysica acta*. 2009;1791(6):399-407.
57. Greenberg AS, Egan JJ, Wek SA, Moos MC, Jr., Londos C, Kimmel AR. Isolation of cDNAs for perilipins A and B: sequence and expression of lipid droplet-associated proteins of adipocytes. *Proceedings of the National Academy of Sciences of the United States of America*. 1993;90(24):12035-9.
58. Martin S, Parton RG. Lipid droplets: a unified view of a dynamic organelle. *Nature reviews Molecular cell biology*. 2006;7(5):373-8.
59. Blanchette-Mackie EJ, Dwyer NK, Barber T, Coxey RA, Takeda T, Rondinone CM, et al. Perilipin is located on the surface layer of intracellular lipid droplets in adipocytes. *Journal of lipid research*. 1995;36(6):1211-26.
60. Londos C, Brasaemle DL, Schultz CJ, Segrest JP, Kimmel AR. Perilipins, ADRP, and other proteins that associate with intracellular neutral lipid droplets in animal cells. *Seminars in cell & developmental biology*. 1999;10(1):51-8.
61. Brasaemle DL, Barber T, Wolins NE, Serrero G, Blanchette-Mackie EJ, Londos C. Adipose differentiation-related protein is an ubiquitously expressed lipid storage droplet-associated protein. *Journal of lipid research*. 1997;38(11):2249-63.
62. Wolins NE, Rubin B, Brasaemle DL. TIP47 associates with lipid droplets. *The Journal of biological chemistry*. 2001;276(7):5101-8.
63. Wolins NE, Skinner JR, Schoenfish MJ, Tzekov A, Bensh KG, Bickel PE. Adipocyte protein S3-12 coats nascent lipid droplets. *The Journal of biological chemistry*. 2003;278(39):37713-21.
64. Dalen KT, Dahl T, Holter E, Arntsen B, Londos C, Sztalryd C, et al. LSDP5 is a PAT protein specifically expressed in fatty acid oxidizing tissues. *Biochimica et biophysica acta*. 2007;1771(2):210-27.
65. Bindesboll C, Berg O, Arntsen B, Nebb HI, Dalen KT. Fatty acids regulate perilipin5 in muscle by activating PPARdelta. *Journal of lipid research*. 2013;54(7):1949-63.
66. Hsieh K, Lee YK, Londos C, Raaka BM, Dalen KT, Kimmel AR. Perilipin family members preferentially sequester to either triacylglycerol-specific or cholesteryl-ester-specific intracellular lipid storage droplets. *Journal of cell science*. 2012;125(Pt 17):4067-76.
67. Brasaemle DL, Rubin B, Harten IA, Gruia-Gray J, Kimmel AR, Londos C. Perilipin A increases triacylglycerol storage by decreasing the rate of triacylglycerol hydrolysis. *The Journal of biological chemistry*. 2000;275(49):38486-93.
68. Yang X, Heckmann BL, Zhang X, Smas CM, Liu J. Distinct mechanisms regulate ATGL-mediated adipocyte lipolysis by lipid droplet coat proteins. *Molecular endocrinology (Baltimore, Md)*. 2013;27(1):116-26.
69. Martinez-Botas J, Anderson JB, Tessier D, Lapillonne A, Chang BH, Quast MJ, et al. Absence of perilipin results in leanness and reverses obesity in *Lepr*(db/db) mice. *Nature genetics*. 2000;26(4):474-9.
70. Tansey JT, Sztalryd C, Gruia-Gray J, Roush DL, Zee JV, Gavrilova O, et al. Perilipin ablation results in a lean mouse with aberrant adipocyte lipolysis, enhanced leptin production, and resistance to diet-induced obesity. *Proceedings of the National Academy of Sciences of the United States of America*. 2001;98(11):6494-9.

71. Chang BH, Li L, Saha P, Chan L. Absence of adipose differentiation related protein upregulates hepatic VLDL secretion, relieves hepatosteatosis, and improves whole body insulin resistance in leptin-deficient mice. *Journal of lipid research*. 2010;51(8):2132-42.
72. Chang BH, Li L, Paul A, Taniguchi S, Nannegari V, Heird WC, et al. Protection against fatty liver but normal adipogenesis in mice lacking adipose differentiation-related protein. *Molecular and cellular biology*. 2006;26(3):1063-76.
73. Wolins NE, Quaynor BK, Skinner JR, Schoenfish MJ, Tzekov A, Bickel PE. S3-12, Adipophilin, and TIP47 package lipid in adipocytes. *The Journal of biological chemistry*. 2005;280(19):19146-55.
74. Lee YK, Sohn JH, Han JS, Park YJ, Jeon YG, Ji Y, et al. Perilipin 3 Deficiency Stimulates Thermogenic Beige Adipocytes Through PPAR α Activation. *Diabetes*. 2018;67(5):791-804.
75. Dalen KT, Schoonjans K, Ulven SM, Weedon-Fekjaer MS, Bentzen TG, Koutnikova H, et al. Adipose tissue expression of the lipid droplet-associating proteins S3-12 and perilipin is controlled by peroxisome proliferator-activated receptor- γ . *Diabetes*. 2004;53(5):1243-52.
76. Chen W, Chang B, Wu X, Li L, Sleeman M, Chan L. Inactivation of Plin4 downregulates Plin5 and reduces cardiac lipid accumulation in mice. *American journal of physiology Endocrinology and metabolism*. 2013;304(7):E770-9.
77. Wolins NE, Quaynor BK, Skinner JR, Tzekov A, Croce MA, Gropler MC, et al. OXPAT/PAT-1 is a PPAR-induced lipid droplet protein that promotes fatty acid utilization. *Diabetes*. 2006;55(12):3418-28.
78. Pollak NM, Schweiger M, Jaeger D, Kolb D, Kumari M, Schreiber R, et al. Cardiac-specific overexpression of perilipin 5 provokes severe cardiac steatosis via the formation of a lipolytic barrier. *Journal of lipid research*. 2013;54(4):1092-102.
79. Granneman JG, Moore HP, Mottillo EP, Zhu Z, Zhou L. Interactions of perilipin-5 (Plin5) with adipose triglyceride lipase. *The Journal of biological chemistry*. 2011;286(7):5126-35.
80. Kuramoto K, Okamura T, Yamaguchi T, Nakamura TY, Wakabayashi S, Morinaga H, et al. Perilipin 5, a lipid droplet-binding protein, protects heart from oxidative burden by sequestering fatty acid from excessive oxidation. *The Journal of biological chemistry*. 2012;287(28):23852-63.
81. Kuramoto K, Sakai F, Yoshinori N, Nakamura TY, Wakabayashi S, Kojidani T, et al. Deficiency of a lipid droplet protein, perilipin 5, suppresses myocardial lipid accumulation, thereby preventing type 1 diabetes-induced heart malfunction. *Molecular and cellular biology*. 2014;34(14):2721-31.
82. Desjardins P, Conklin D. NanoDrop microvolume quantitation of nucleic acids. *Journal of visualized experiments : JoVE*. 2010(45).
83. Haddad F, Baldwin KM. Reverse Transcription of the Ribonucleic Acid: The First Step in RT-PCR Assay. In: King N, editor. *RT-PCR Protocols: Second Edition*. Totowa, NJ: Humana Press; 2010. p. 261-70.
84. Livak KJ, Schmittgen TD. Analysis of relative gene expression data using real-time quantitative PCR and the 2⁻($\Delta\Delta C_T$) Method. *Methods (San Diego, Calif)*. 2001;25(4):402-8.
85. Khan-Malek R, Wang Y. Statistical Analysis of Quantitative RT-PCR Results. *Methods in molecular biology (Clifton, NJ)*. 2017;1641:281-96.
86. Valente V, Teixeira SA, Neder L, Okamoto OK, Oba-Shinjo SM, Marie SK, et al. Selection of suitable housekeeping genes for expression analysis in glioblastoma using quantitative RT-PCR. *BMC molecular biology*. 2009;10:17.

87. Spangenburg EE, Pratt SJP, Wohlers LM, Lovering RM. Use of BODIPY (493/503) to visualize intramuscular lipid droplets in skeletal muscle. *Journal of biomedicine & biotechnology*. 2011;2011:598358.
88. Hariharan D, Vellanki K, Kramer H. The Western Diet and Chronic Kidney Disease. *Current hypertension reports*. 2015;17(3):16.
89. Browning JD, Baxter J, Satapati S, Burgess SC. The effect of short-term fasting on liver and skeletal muscle lipid, glucose, and energy metabolism in healthy women and men. *Journal of lipid research*. 2012;53(3):577-86.
90. Edvardsson U, Ljungberg A, Linden D, William-Olsson L, Peilot-Sjogren H, Ahnmark A, et al. PPARalpha activation increases triglyceride mass and adipose differentiation-related protein in hepatocytes. *Journal of lipid research*. 2006;47(2):329-40.
91. Dalen KT, Ulven SM, Arntsen BM, Solaas K, Nebb HI. PPARalpha activators and fasting induce the expression of adipose differentiation-related protein in liver. *Journal of lipid research*. 2006;47(5):931-43.
92. Griessl M, Gutknecht M, Cook CH. Determination of suitable reference genes for RT-qPCR analysis of murine Cytomegalovirus in vivo and in vitro. *Journal of virological methods*. 2017;248:100-6.
93. Yuzbasioglu A, Onbasilar I, Kocaeffe C, Ozguc M. Assessment of housekeeping genes for use in normalization of real time PCR in skeletal muscle with chronic degenerative changes. *Experimental and molecular pathology*. 2010;88(2):326-9.
94. Nakao R, Okauchi H, Hashimoto C, Wada N, Oishi K. Determination of reference genes that are independent of feeding rhythms for circadian studies of mouse metabolic tissues. *Molecular genetics and metabolism*. 2017;121(2):190-7.
95. Tatsumi K, Ohashi K, Taminishi S, Okano T, Yoshioka A, Shima M. Reference gene selection for real-time RT-PCR in regenerating mouse livers. *Biochemical and biophysical research communications*. 2008;374(1):106-10.
96. Gong H, Sun L, Chen B, Han Y, Pang J, Wu W, et al. Evaluation of candidate reference genes for RT-qPCR studies in three metabolism related tissues of mice after caloric restriction. *Scientific reports*. 2016;6:38513.
97. geNorm. geNorm normalization of real-time PCR expression data 2018 [updated 06.09.18. Available from: <https://genorm.cmgg.be>.
98. BiteSize Bio. Tissue embedding throwdown, Paraffin vs OCT vs Resin 2017 [Available from: <https://bitesizebio.com/35317/tissue-embedding/>.
99. Hagan IM. Staining Fission Yeast Filamentous Actin with Fluorescent Phalloidin Conjugates. *Cold Spring Harbor protocols*. 2016;2016(6).
100. Feng YZ, Lund J, Li Y, Knabenes IK, Bakke SS, Kase ET, et al. Loss of perilipin 2 in cultured myotubes enhances lipolysis and redirects the metabolic energy balance from glucose oxidation towards fatty acid oxidation. *Journal of lipid research*. 2017;58(11):2147-61.
101. Kirkwood BRS, J.A.C; . *Essential Medical Statistics Second edition*, ed. Malden, Massachusetts, USA Blackwell Science Ltd 2003.
102. Bell M, Wang H, Chen H, McLenithan JC, Gong DW, Yang RZ, et al. Consequences of lipid droplet coat protein downregulation in liver cells: abnormal lipid droplet metabolism and induction of insulin resistance. *Diabetes*. 2008;57(8):2037-45.

Appendix

Appendix 1. Specific primer-pairs used for RT-qPCR

Gene name	Forward primer	Reverse primer	Accession	Product size	Intron length
Abca1	ACCGAGGAAGAAGCT CGATG	GGTCGGGAGATGAGA TGTGG	NM_01345 4.3	103	11328
Abcg1	AAGGTCTCCAATCTC GTGCC	CCCTGATGCCACTTCC ATGA	NM_00959 3.2	96	2131
ApoE	CCTGAACCGCTTCTG GGATT	CCATCAGTGCCGTCAG TTCT	NM_00969 6.4	107	414
Chrebp	TGCAGCCCAGCCTAG ATGAC	AGCTGGGGGACTCTAT GTAGTT	NM_02145 5.4	102	4495
Dgat1	CCATACCCGGGACAA AGACG	GAATCTTGACAGACGAT GGCAC	NM_01004 6.2	78	4901
Dgat2	GGCTACGTTGGCTGG TAACT	ATGGTGTCTCGGTTGA CAGG	NM_02638 4.3	87	505
Fasn	CTTCGGCTGCTGTTGG AAGTC	GTGTTCTGTTCCCTCGGA GTGAG	NM_00798 8.3	80	1005
Ldlr	GACTGCAAGGACATG AGCGA	TGTCCAAGCTGATGCA CTCC	NM_01070 0.3	103	1860
Lpl	CGCTCTCAGATGCCCT ACAA	CTGGTTGTGTTGCTTG CCAT	NM_00850 9.2	84	2575
LXRα	GACTTCAGTTACAAC CGGGAAGA	ATTCATGGCTCTGGAG AACTCAA	NM_00117 7730.1	90	5129
LXRβ	GAAGGCGTCCACCAT TGAG	AAGTCGTCCTTGCTGT AGGT	NM_00128 5517.1	108	473
Plin1	ACCTGGAGGAAAAGA TCCCG	TTCGAAGGCGGGTAG AGATG	NM_00111 3471.1	87	1316
Plin2	GGGCTAGACAGGATG GAGGA	CACATCCTTCGCCCCA GTTA	NM_00740 8.3	99	2215
Plin3	CGAAGCTCAAGCTGC TATGG	TCACCATCCCATACGT GGAAC	NM_02583 6.3	98	1147
Plin4	ACCAACTCACAGATG GCAGG	AGGCATCTTCACTGCT GGTC	NM_02056 8.3	109	1213
Plin5	GGTGAAGACACCACC CTAGC	CCACCACTCGATTAC CACA	NM_00107 7348.1	115	568
PPARα	ACTACGGAGTTCACG CATGT	GTCGTACACCAGCTTC AGCC	NM_00111 3418.1	74	1710
PPARγ	CGGGCTGAGAAGTCA CGTT	TCAGTGTTTACCGCT TCTTT	NM_00112 7330.1	70	22308
Srebf1a	GGCCGAGATGTGCGA ACTG	GTTGTTGATGAGCTGG AGCATGT	NM_00131 3979.1	70	13195
Srebf1c	GGAGCCATGGATTGC ACATTT	CAGCATAGGGGGCGT CAAA	XM_00653 2716.2	91	3078
Srebf2	TGACTCTCGGGGACA TCGAC	CACCTCCAGGGAAGG AGCTA	NM_03321 8.1	105	22247
Tbp	AGCCTTCCACCTTATG CTCAG	GCCGTAAGGCATCATT GGACT	NM_01368 4.3	90	1145